Journal of Clinical and Translational Research

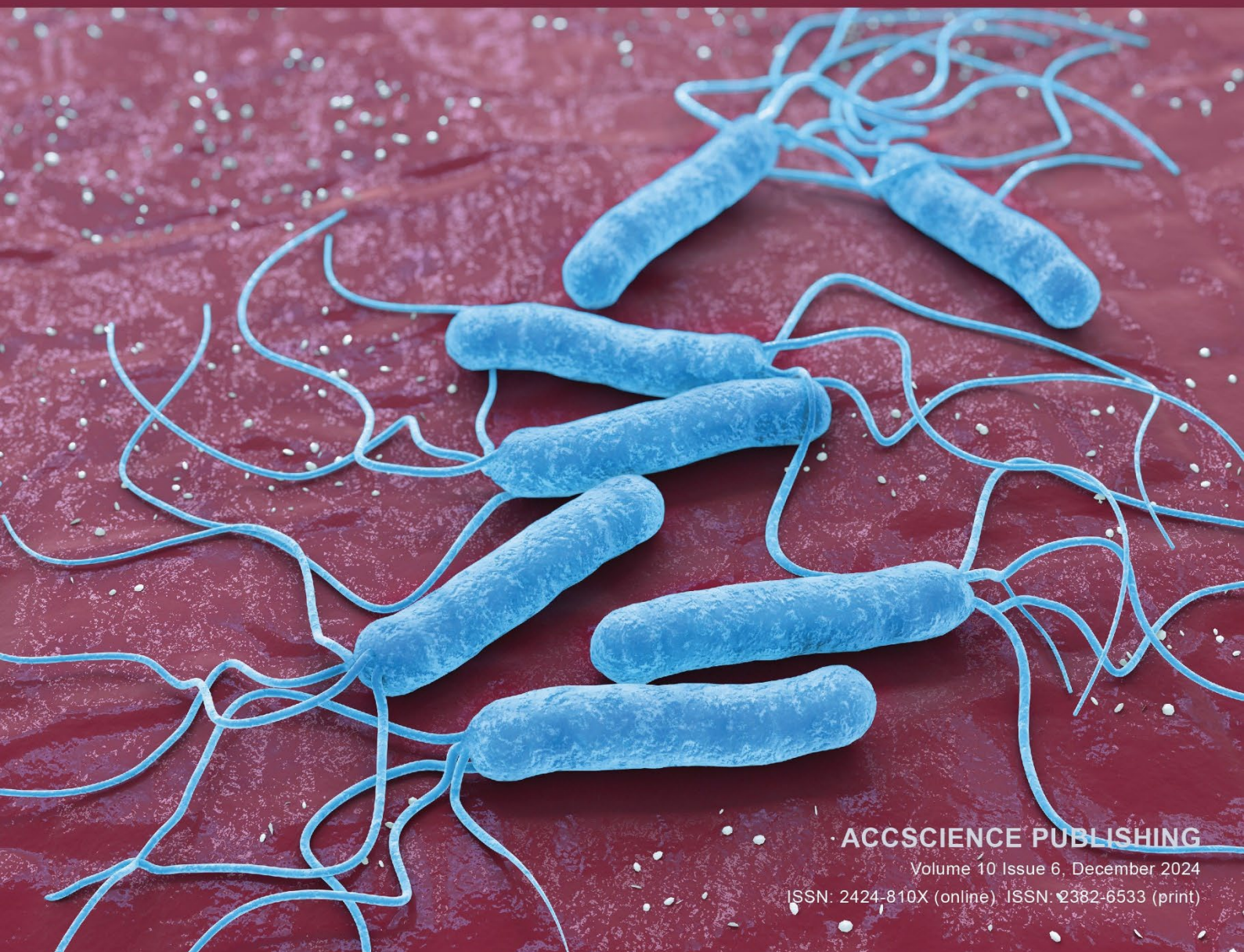

ACCSCIENCE PUBLISHING
Volume 10 Issue 6, December 2024
ISSN: 2424-810X (online) ISSN: 2382-6533 (print)

ABOUT JCTR

Aims and scope

The Journal of Clinical and Translational Research (JCTR) is an open access, peer-reviewed, multidisciplinary scientific journal that publishes studies with at least an ex vivo, in vivo, or clinical component. The published research is centered on any clearly defined clinical problem, which may comprise a disease or the basis of disease, a form of therapy or intervention, and clinical diagnostics or prognostics. Articles (original research, reviews, technical reports, medical hypotheses, commissioned articles, special issue articles, and editorials) are published continuously online and bimonthly in print. Studies performed in cells only will generally not be accepted unless they contain critical data that are in line with the scope of the journal. Some examples of such studies include molecular pathways that lie at the basis of a disease, novel biotechnological approaches for e.g., the production of drugs, or new techniques that improve clinical diagnostics and prognostics. Articles that combine preclinical and clinical data are given priority. Contributions from academic institutions and industry are welcome.

The research areas that JCTR covers include but are not limited to:

Internal medicine (all branches)
Vascular medicine and phlebology
Oncology
Cardiology
Intensive care medicine
Ophthalmology
Neurology and neurosciences
Anatomy, physiology, and embryology
Pathology
Clinical physics
Epidemiology
Medical devices
Pharmacology
Microbiology
Parasitology
Biomedical spectroscopy and spectrometry
Gastroenterology and hepatology
Surgery and transplantation
Hematology
Nephrology
Dermatology
Endocrinology and metabolism
Anesthesiology
Radiology and nuclear medicine
Clinical chemistry
Genetics and epigenetics
Global health
Nutrition
Immunology
Virology
Biomedical engineering

Key features

- Open access
- Reputable international editorial board
- Easy and fast submissions - no formatting rules (“your paper, your way”)
- No word count or reference restrictions
- Double blind review process to minimize bias
- Rapid online publication of articles upon acceptance
- Outlet for academic institutions and industry

Indexing

The Journal of Clinical and Translational Research is currently indexed by Chemical Abstract Service, Google Scholar, CNKI, and Peking University Library, and is currently working towards being indexed (PubMed, Science Citation Index Expanded, BIOSIS, Scopus, etc.).

Volume 10 • Issue 6 • December 2024
ISSN 2382-6533 (print) ISSN 2424-810X (online)

JOURNAL OF CLINICAL AND TRANSLATIONAL RESEARCH

ACCSCIENCE PUBLISHING

Journal of Clinical and Translational Research

Editorial Board

ACCSCIENCE PUBLISHING

Volume 10 | Issue 6 | December 2024 | Page 317 – 356 |

Journal of Clinical and Translational Research

https://www.jctres.com/en/home/

CONTENTS

CONTACTS

For general inquiries about the journal
y.liu@jctres.com (Dr. Yao Liu)

For ethical/legal inquiries
y.liu@jctres.com (Dr. Yao Liu)

For translation and proofreading services (English)
y.liu@jctres.com (Dr. Yao Liu)

For manuscript production inquiries
production@jctres.com

For advertisement inquiries
y.liu@jctres.com (Dr. Yao Liu)

Other Journal Published by AccScience Publishing

International Journal of Bioprinting is an international journal covering the technology, science and clinical application of the broadly defined field of bioprinting. Bioprinting is defined as the use of 3D printing technology with materials that incorporate viable living cells or biological elements to produce tissue or biotechnological products.

We are interested in the scientific topics spanning all stages of bioprinting process from concept creation to fabrication and beyond. Knowledge generated in these researches must be related to bioprinting.

The journal publishes original research articles on basic and applied research as well as associated social implications of this research. The journal also publishes brief commentaries and reviews. Articles focusing on the practical applications of 3D-printed products are similarly welcome.

Journal of Clinical and Translational Research 2024; 10(6): 317-324

Journal of Clinical and Translational Research

Journal homepage: http://www.jctres.com/en/home

ORIGINAL ARTICLE

Efficacy and safety of vonoprazan as a component of the first- and second-line eradication regimens for *Helicobacter pylori*: a real-life Egyptian study

Abdelfattah Hanno[1], Magdy El-Dahshan[2], Tarek Youssef[3], Ali Farag[4], Hussein Elamin[5], Magdi Hamed[6], Sherief Abdel-Salam[7], Ehab Abdelatty[8], Eman Abdelsameea[9]*, Yasser Fouad[10], Shamardan Ezz-Eldin[11], Waleed A. Abd El Dayem[12], Ebada Said[13], Mohamed S. Ahmed[1]

[1]Department of Tropical Medicine, Faculty of Medicine, Alexandria University, Alexandria, Egypt, [2]Department of Internal Medicine, Hepatogastroenterology Unit, Faculty of Medicine, Al-Azhar University, Cairo, Egypt, [3]Department of Internal Medicine and Hepatogastroenterology, Faculty of Medicine, Ain Shams University, Cairo, Egypt, [4]Department of Internal Medicine, Gastroenterology Unit, Faculty of Medicine, Cairo University, Cairo, Egypt, [5]Department of Internal Medicine, Gastroenterology Unit, Faculty of Medicine, Assiut University, Assiut, Egypt, [6]Department of Hepatogastroenterology, Faculty of Medicine, Mansoura University, Mansoura, Egypt, [7]Department Internal Medicine, Gastroenterology Unit, Faculty of Medicine, Tanta University, Gharbia, Egypt, [8]Department of Internal Medicine, Hepatology and Gastroenterology Unit, Faculty of Medicine, Menofia University, Menofia, Egypt, [9]Department of Hepatology and Gastroenterology, National Liver Institute, Menoufia University, Shebin El-Kom, Egypt, [10]Department of Tropical Medicine, Faculty of Medicine, Minia University, Minia, Egypt, [11]Department of Tropical Medicine and Gastroenterology, Faculty of Medicine, South Vally University, Qena, Egypt, [12]Hepatogastroenterology and Infectious Disease Department, Faculty of Medicine, Zagazig University, Sharkia, Egypt, [13]Department of Hepatology, Gastroenterology and Infectious Diseases, Benha University, Qalyubia, Egypt

ARTICLE INFO

Article history:
Received: July 13, 2024
Accepted: October 25, 2024
Published Online: November 26, 2024

Keywords:
Vonoprazan
Proton-pump inhibitor
Helicobacter pylori

**Corresponding author:*
Eman Abdelsameea
Department of Hepatology and Gastroenterology, National Liver Institute, Menoufia University, Shebin El-Kom, Egypt.
Email: eabdelsameea@liver-eg.org

ABSTRACT

Background: Vonoprazan, a new potassium competitive acid blocker, offers a rapid onset of action and a predictable antisecretory profile that is independent of the CYP2C19 genotype or parietal cell activity. This profile may enhance *Helicobacter pylori* eradication therapy.
Aim: This research compared vonoprazan and proton-pump inhibitors (PPI) in Egypt's first- and second-line *H. pylori* eradication regimens for effectiveness, safety, and tolerability.
Methods: A prospective, controlled, multicenter, parallel-assignment, and open-label study was designed to verify the superiority of vonoprazan versus PPI in first-line therapy (with amoxicillin and clarithromycin) or second-line therapy (with levofloxacin, doxycycline, and nitazoxanide) for *H. pylori* eradication. Patients received either vonoprazan- or PPI-based regimens for 14 days followed by a 4-week follow-up period. The primary efficacy endpoint is the rate of first-line eradication, while the secondary endpoint is the rate of second-line eradication among individuals who did not respond to first-line treatment. Safety and tolerability of both first- and second-line treatments were also assessed.
Results: Of the 1184 patients allocated to the study, 701 naïve patients received first-line therapy (355 patients received a triple vonoprazan-based regimen; 346 patients received triple PPI-based regimen), and 483 experienced patients received the second-line therapy (243 patients received quadrable vonoprazan-based regimen and 240 patients received quadrable PPI-based regimen). The first-line eradication rate was 91% in vonoprazan triple therapy versus 74.6% in PPI triple therapy ($P < 0.001$). The second-line eradication rate was 89.7% in vonoprazan quadrable therapy versus 78.3% in PPI quadrable therapy ($P < 0.001$). Both first- and second-line therapies were well tolerated with no remarkable adverse events or safety outcomes.
Conclusion: In both naive and experienced patients, vonoprazan-based treatment was statistically and substantially superior to omeprazole-based therapy in eradicating *H. pylori*.
Relevance for Patients: This work offers a promising approach for the treatment of Egyptian patients with *H. pylori* infection.

DOI: http://doi.org/10.36922/jctr.24.00043

1. Introduction

Helicobacter pylori, a Gram-negative, microaerobic human pathogen, is linked to non-cardia stomach cancer, chronic active gastritis, peptic ulcer disease (PUD), atrophic gastritis, and mucosa-associated lymphoid tissue (MALT) lymphoma. *H. pylori* infects almost half of the adult population worldwide, though it is prevalent across geographies, races, ages, and socioeconomic groups [1,2].

Most of those infected with *H. pylori* will develop either gastric (70 – 90%) or duodenal (90%) ulcers [3]. However, some with *H. pylori* infection remain asymptomatic [4].

Non-cardiac stomach cancer is the third most frequent cause of cancer deaths worldwide, with *H. pylori* responsible for 74.7% of cases. *H. pylori* infection remains a critical issue, contributing to stomach cancer and ulcers, which together cause over a million deaths worldwide annually [1].

Screening and treatment are needed for active *H. pylori* infections. Individuals with ongoing or a history of PUD (unless previously treated), low-grade MALT lymphoma, endoscopic excision of early gastric cancer, or individuals under 60 years old with unexplained dyspepsia and no warning symptoms should be tested for *H. pylori* [5].

H. pylori diagnosis requires tests with >90% sensitivity and specificity. Managing numerous gastroduodenal disorders requires accurate *H. pylori* diagnosis. Histological, culture, and fast urease tests require endoscopy and biopsy, whereas serology, urea breath test, and stool antigen detection do not [1].

A global meta-analysis found the stool antigen test (SAT) to be 94% sensitive and 97% specific for *H. pylori* infection. This method detected *H. pylori* antigen in feces. Antibiotics, proton-pump inhibitors (PPI), N-acetylcysteine, diarrhea, and gastrointestinal (GI) bleeding can impact SAT accuracy [1].

Polyclonal antibodies and monoclonal antibodies are utilized in either enzyme immunoassay (EIA)- or immunochromatography-based SATs for *H. pylori* detection. The monoclonal SAT is a quick, painless, and accurate way to determine if you have a current *H. pylori* infection. The EIA test, which detects anti-*H. pylori* IgG antibodies, is the most common and effective serological test for *H. pylori* [1].

Serological tests are unaffected by ulcers, bleeding, stomach atrophy, PPIs, or antibiotics, unlike other invasive and non-invasive investigations. Due to their low cost, speed, and patient acceptability, serological tests have been routinely employed as a screening tool in epidemiological investigations. Even after effective eradication, antibody levels in the blood can remain elevated for extended durations, making the serological test an unreliable method of evaluation [6].

H. pylori is an infectious disease treated with 2 – 3 antibiotics and PPI for 3 – 14 days [4]. Increasing intragastric pH with a PPI and two antibiotics eliminates *H. pylori*; when the intragastric pH exceeds 5, *H. pylori* can grow and become more antibiotic-sensitive [7,8].

A rise in antibiotic-resistant genotypes of *H. pylori* has contributed to a decline in recent *H. pylori* eradication rates, despite the continued use of conventional PPIs to inhibit gastric acid secretion [9].

The fast evolution of antibiotic-resistant *H. pylori* strains has a significant impact on the efficacy of eradication treatment. Antibiotic resistance is an ever-changing process, and the incidence of *H. pylori* antibiotic resistance varies greatly between countries, and even in areas within the same country [10]. The most recent agreement for *H. pylori* care in Egypt suggested the same first- and second-line medications as the worldwide recommendations [11]; however, numerous studies recommend identifying *H. pylori* antibiotic resistance.

Metwally *et al*. [12] mentioned that in Egyptian patients, *H. pylori* demonstrated more than 90% resistance to metronidazole and amoxicillin (AMO); minor resistance to erythromycin, azithromycin, and clarithromycin (CLA); and low resistance to moxifloxacin and levofloxacin (≤20%). Dual resistance was high for AMO/CLA and AMO/metronidazole, indicating that quinolones are preferred over CLA or metronidazole for first-line *H. pylori* therapy in Egypt.

To enhance eradication efficiency, antibiotics have been changed, and PPI doses have been increased. The increased rate of eradication promotes the production of potassium competitive acid blockers (P-CABs), a chemical that decreases acid output [13].

Similar to PPIs, the new oral P-CAB vonoprazan inhibits gastric H^+-K^+-ATPase, the enzyme responsible for the final step of stomach acid production [14]. In contrast to PPIs, vonoprazan inhibits the enzyme in a K^+-competitive and reversible manner [15].

To effectively eradicate an *H. pylori* infection, nighttime stomach acid suppression must be maintained over an extended period. The optimal pH range when the organism is growing and sensitive to antibiotics (e.g., CLA and AMO) is 6 – 7 [16]. Acid suppression achieved by currently available PPIs is often insufficient, both in terms of magnitude and duration, to reach this level throughout the entire 24-h period. However, P-CABs are most effective when used in conjunction with one or more antimicrobial drugs, due to their unique pharmacological profile [17,18].

There is no correlation between CYP2C19 genotype and parietal cell activation, and P-CABs have a rapid onset of action and a predictable anti-secretory profile. In particular, this profile has the potential to simplify complex eradication regimens and pave the way for the development of highly effective dual therapy, both of which would lead to better *H. pylori* treatment management [18,19].

Furthermore, research has demonstrated that vonoprazan (pKa: 9.4) accumulates in parietal cells and that the pH of the surrounding environment has little impact on its acid-inhibitory effect [20,21]. Vonoprazan administered in multiple doses (10 – 40 mg/day) for 7 days in healthy volunteers maintained the dose-dependent, potent, and rapid acid inhibitory effects observed at 24 h compared to single doses (10 – 20 mg) [22,23]. Vonoprazan is likely to be as effective as PPIs in *H. pylori* treatment due to its stronger acid inhibition [24].

Here, this study aimed to assess the effectiveness, safety, and tolerability of vonoprazan in combination with PPI in Egyptian patients for the treatment of *H. pylori*.

DOI: http://doi.org/10.36922/jctr.24.00043

2. Methods

2.1. Study design

This was a prospective, controlled, multicenter, parallel-assignment, and open-label study involving patients selected from the gastroenterology and/or tropical medicine departments, as well as inpatient and outpatient clinics, from 12 university centers across Egypt (i.e., Faculty of Medicine of Alexandria University, Al-Azhar University, Ain Shams University, Cairo University, Assiut University, Mansoura University, Tanta University, Minia University, South Valley University, Zagazig University, Benha University; Faculty of Medicine and National Liver Institute of Menoufia University). The study was conducted from January 1, 2022, to June 30, 2022.

The inclusion criteria were patients (i) above 18 years of matched age and sex, and (ii) provided written informed consent before study participation. The exclusion criteria were patients (i) with known allergy to any of the treatment drugs; (ii) refused to sign an informed consent; (iii) had surgery that might affect gastric acid secretion (upper GI resection or vagotomy), Zollinger–Ellison syndrome, or other gastric acid hypersecretion disorders; (iv) had serious neurological, cardiovascular, pulmonary, hepatic, renal, metabolic, GI, urological, endocrinological, or hematological disorders; (v) need surgery, history of drug (including alcohol) abuse, history of malignancy, and female subjects who are pregnant or lactating; (vi) pregnancy or planning for pregnancy during the study period; and (vii) on PPIs, P-CABs, and/or antibiotics within 1 month before inclusion in the study.

Patients who fulfilled the study inclusion criteria were allocated to one group of study as follows:

(i) Group-I: Naïve patients (patients who did not receive any prior *H. pylori* eradication regimens)
   - Arm 1: Patients received vonoprazan triple therapy: CLA 500 mg twice daily (bis in die [BID]) + AMO 1 g BID + vonoprazan 20 mg BID for 14 days
   - Arm 2: Patients received the classic triple therapy: CLA 500 mg BID + AMO 1 g BID + PPI "omeprazole 40 mg" BID for 14 days

(ii) Group-II: Non-responders (patients who did not respond to the previous first-line eradication regimen):
   - Arm 1: Patients received vonoprazan-based non-bismuth quadruple therapy: levofloxacin 500 mg once daily (OD) + vonoprazan 20 mg BID + nitazoxanide 500 mg BID + doxycycline 100 mg OD for 14 days
   - Arm 2: Patients received the classic non-bismuth quadruple therapy: Levofloxacin 500 mg OD + PPI "omeprazole 40 mg" BID + nitazoxanide 500 mg BID + doxycycline 100 mg OD) for 14 days.

2.2. Data collection

A total of 1200 patients were enrolled at the beginning of the study and were further divided into two equal-sized groups, each containing 600 subjects. The subjects were blindly allocated to vonoprazan and traditional PPI therapies. At the end of the study, two patients from the vonoprazan group did not complete the study, and 14 patients from the PPI group voluntarily stopped the drug regimen and did not complete the study.

The final sample size was 1184 patients, and they were divided accordingly in the study: 701 naïve patients received first-line therapy (355 patients received a triple vonoprazan-based regimen, and 346 patients received a triple PPI-based regimen), and 483 experienced patients received the second-line therapy (243 patients received quadrable vonoprazan-based regimen, and 240 patients received quadrable PPI-based regimen). After recruitment and allocation, all patients were subjected to the following:

(i) Full history and complete clinical examination: stool analysis, urine, complete blood count, *H. pylori* antigen (Ag) in stool (quantitative assay), and serum creatinine.

(ii) The presence of *H. pylori* was confirmed by the *H. pylori* SAT before study treatment administration and 4 weeks after the treatment regimen; antibiotics and acid-suppressive therapies were discontinued 2 weeks before doing the test.

During follow-ups, the patients were contacted by telephone after 1 week of starting the regimen to check compliance. The first follow-up visit was after completing 2 weeks of treatment to register any adverse events. The second follow-up visit was after completing 4 weeks of the treatment regimen to register the eradication results.

The primary purpose of the trial was to increase the rate of first-line *H. pylori* elimination. The second endpoint was the rate of H. pylori elimination in those who failed the first line of therapy.

The incidence of treatment-emergent adverse events was recorded. The principal investigator supervised the assessment of the safety of triple and quadrable therapy for *H. pylori* eradication in the local population.

2.3. Statistical analysis

The sample size was calculated using Power Analysis and Sample Size software (PASS 2020; ncss.com/software/pass; NCSS, LLC., USA). The minimal total hypothesized sample size of 800 eligible patients (400 per group) is required to compare the efficacy of vonoprazan and PPI in Egypt's first- and second-line *H. pylori* eradication regimens. This calculation assumes a 25% effect size (i.e., a minimally clinically important difference), a 95% confidence level, a 1:1 compliance ratio, and 80% power, using the Chi-square test [25,26]. The sample size was estimated based on the formula:

$$Sample\ size\ (n) = N \times \frac{[\frac{Z2 \times p \times (1-p)}{e2}]}{N-1+[\frac{Z2 \times p \times (1-p)}{e2}]} \quad (I)$$

Where N is the population size, Z is the critical value of the normal distribution at the required confidence level, p is the sample proportion, and e is the margin of error.

Data were fed to the computer and analyzed using IBM Statistical Package for the Social Sciences software version 20.0 (IBM Corp., USA). A Chi-square test was applied to compare

DOI: http://doi.org/10.36922/jctr.24.00043

different categories. The significance of the obtained results was judged at the 5% level.

3. Results

Table 1 presents the age of the participants; most participants (33.3%) aged 20 – 30 years, while the smallest percentage (0.3%) aged over 70 years. Moreover, female participants slightly outnumbered male participants (50.3% vs. 49.7%, respectively). There were also more naïve patients than experienced patients (58.5% vs. 41.5%, respectively).

Table 2 indicates that vonoprazan-based treatment outperformed omeprazole-based therapy in eradicating *H. pylori* in both naïve ($P < 0.001$) and experienced ($P = 0.001$) patients. However, vonoprazan-based treatment did not significantly vary between naïve and experienced groups ($p_0 = 0.504$).

Table 3 documents the adverse events experienced by patients. From the 598 vonoprazan-treated patients, five reported nausea/vomiting, ten with diarrhea, eight with constipation, two with bloating, and six with rashes, but none of them were severe.

Table 4 shows different regimens for previous Helicobacter pylori treatment. Among the 483 experienced patients, 119 (24.64%) of them received PPI, amoxicillin and clarithromycin, and 154 (31.88%) patients received PPI, amoxicillin and quinolones.

4. Discussion

Vonoprazan was just recently brought to the Egyptian market in early 2022, though it has been available in Japan and a few other nations since 2015. This is the first multicentric Egyptian study of vonoprazan triple therapy for *H. pylori*.

Standard triple treatment (STT) with PPIs, AMO, and CLA is unsuccessful in many countries due to *H. pylori* developing CLA resistance. Four-drug combinations, such as bismuth-containing quadruple therapy (BQT) or concurrent quadruple therapy, are first-line therapies for such diseases [27,28].

In previous studies, the eradication rates were 55 – 72% for STT within 7 days [25,29], 80 – 95% for BQT [30,31], and 86 – 91% for concomitant quadruple therapy (CQT) [32] as first-

Table 1. Distribution of the studied cases according to different parameters (n=1184)

Parameter	Number of patients (%)			Test of significance	*P*-value
	Total (n=1184) (%)	Group I (n=586) (%)	Group II (n=598) (%)		
Age (years)					
20 – 30	394 (33.3)	203 (34.6)	191 (31.9)	χ^2=7.934	0.160
31 – 40	353 (29.8)	179 (30.5)	174 (29.1)		
41 – 50	236 (19.9)	120 (20.5)	116 (19.4)		
51 – 60	149 (12.6)	63 (10.8)	86 (14.4)		
61 – 70	49 (4.1)	21 (3.6)	28 (4.7)		
>70	3 (0.3)	0 (0)	3 (0.5)		
Sex					
Male	589 (49.7)	300 (51.2)	289 (48.3)	χ^2=0.973	0.324
Female	595 (50.3)	286 (48.8)	309 (51.0)		
Weight (kg)					
Min-Max	69.0 – 121.0	69.0 – 121.0	69.0 – 121.0	t=0.672	0.502
Mean±SD	92.13±15.0	92.72±14.84	92.13±15.0		
Median (IQR)	95.0 (78 – 105)	96.0 (78 – 105)	95.0 (78 – 105)		
Height (cm)					
Min–Max	150.0 – 188.0	150.0 – 188.0	150.0 – 188.0	t=0.034	0.973
Mean±SD	170.06±10.67	170.0±10.59	170.1±10.67		
Median (IQR)	172.0 (161 – 180)	172.0 (161 – 179)	172.0 (161 – 180)		

χ^2 refers to the Chi-square test; t refers to Student's t-test; p refers to the p-value obtained from comparing groups I and II. Abbreviations: SD: Standard deviation; IQR: Interquartile range

Table 2. Comparison between omeprazole- and vonoprazan-based therapy in naïve and experienced patients

Patients	Number of patients (%)		*P*	p_0	
	Omeprazole (%)	Vonoprazan (%)		Omeprazole	Vonoprazan
Naïve (n=701)				0.293	0.504
Positive	88 (25.4)	32 (9.0)	<0.001*		
Negative	258 (74.6)	323 (91.0)			
Experienced (n=483)					
Positive	52 (21.7)	25 (10.3)	0.001*		
Negative	188 (78.3)	218 (89.7)			

"Positive" and "Negative" refer to the drug effect experienced by the patients; *P* denotes *P*-value from the Chi-square test comparing omeprazole- and vonoprazan-based therapy; p_0 denotes *P*-value from the Chi-square test comparing naïve and experienced patients; *denotes statistical significance at P<0.05

DOI: http://doi.org/10.36922/jctr.24.00043

Table 3. Adverse events of vonoprazan-based triple therapy versus conventional proton-pump inhibitor (PPI)-based triple therapy

Adverse effect	Number of patients (%)	
	Vonoprazan (*n*=598) (%)	Conventional PPI (*n*=586) (%)
Rash	6 (1.003)	7 (1.19)
Constipation	8 (1.33)	9 (1.5)
Diarrhea	10 (1.6)	11 (1.8)
Nausea and vomiting	5 (0.8)	3 (0.5)
Bloating	2 (0.3)	1 (0.17)

Table 4. Regimen for previous *Helicobacter pylori* treatment (*n*=483)

Regimen	Number of patients (%)
PPI+amoxicillin+clarithromycin	119 (24.64)
PPI+amoxicillin+quinolones	154 (31.88)
PPI+amoxicillin+metronidazole	117 (24.22)
PPI+amoxicillin+nitazoxanide+clarithromycin	93 (19.26)

Abbreviation: PPI: Proton-pump inhibitor

line *H. pylori* eradication treatments. The vonoprazan, AMO, and CLA triple treatment had eradication rates equivalent to the BQT and CQT and higher than the 7-day STT rate in this study.

We found that vonoprazan-based triple treatment had a higher eradication rate than PPI-based triple therapy as a first-line regimen in naïve patients (91% vs. 74.6%) and as rescue therapy in experienced patients (89.7% vs. 78.3%) in this study.

Consistent with previous findings, vonoprazan-based triple therapy achieved eradication rates exceeding 90%, while PPI-based triple therapy achieved rates of 80% [33]. The triple therapy that includes vonoprazan is preferable because its acid-inhibitory effect is more rapid, potent, and stable [34], and its pharmacokinetic features are not affected by CYP2C19 polymorphism [23].

Dual vonoprazan-AMO and CLA triple treatment eradication rates may be high because the strain infecting participants was not AMO resistant. Despite AMO resistance being lower than other antibiotics, it is often overlooked in *H. pylori* treatments. AMO resistance rates are 38% in Africa, 14% in the Eastern Mediterranean, 12% in Southeast Asia, 8% in the Americas, and 0 – 1% in Europe and the Western Pacific, though it varies significantly in other regions [35].

After 7 days of triple treatment, high-dose PPIs eliminated *H. pylori* infection more effectively compared to conventional doses (82% vs. 74%; 95% confidence interval [CI]: 1.01 – 1.17) in a previous meta-analysis [36]. Increased stomach pH may cause *H. pylori* to re-replicate and become antibiotic-sensitive [9]. If CLA resistance is >15%, many guidelines recommend avoiding PPI-CLA triple therapy [37]. Notably, 40% of patients in Egypt are resistant to CLA [12].

However, PPI-CLA triple therapy is frequently employed in the absence of CLA susceptibility testing, as empirical treatment is less time-consuming and less expensive than testing. Vonoprazan-CLA triple treatment eliminated CLA resistance more effectively than PPI-CLA triple therapy (82.0% vs. 40.0%; 95% CI: 3.63 – 12.86), demonstrating an acceptable eradication rate (i.e., >80%) [38].

When there is no CLA susceptibility test, vonoprazan-CLA triple therapy may be advised empirically. For 14 days, we compared vonoprazan-AMO-CLA treatment to PPI-based therapy for naïve patients and evaluated vonoprazan, nitazoxanide, levofloxacin, and doxycycline to a comparable PPI regimen for experienced patients. Our findings were similar to Mahrous *et al*., who did a similar study on Egyptian patients and compared the effects of vonoprazan, although with a smaller number of patients, included only one center, and used metronidazole instead of CLA in the naïve patients [39].

Our study included only adult participants and did not assess the effect of the drug in children with *H. pylori*. In addition, only three patients over 70 years old were included; hence, further studies are warranted to confirm the efficacy of vonoprazan in children and older adults, especially those with multiple medications and comorbidities.

The drug was well tolerated, with diarrhea being the most reported side effect. This may be linked to the use of CLA, which is known to stimulate GI motility. This finding contrasts with Furuta *et al*., who reported a higher incidence of diarrhea and other side effects with vonoprazan, potentially due to ethnic differences [40].

Nonetheless, this study had limitations, with the primary challenge being how to effectively communicate with the large number of patients and ensure their adherence and compliance to the treatment regimen.

5. Conclusion

In both naive and experienced patients, vonoprazan-based treatment was statistically substantially superior to omeprazole-based therapy in eradicating *H. pylori*. However, the effectiveness of vonoprazan-based treatment was not significantly different between naïve and experienced groups. Therefore, it appears to be a potentially safe and effective *H. pylori* treatment for our Egyptian patients, who tolerated it with few adverse effects.

Acknowledgments

The authors would like to thank all of the patients who participated in this research, the American Journal Experts for copyediting this manuscript, and the Inspire Pharmaceutical Company for funding this study.

Funding

This study was funded by Inspire Pharmaceutical Company (grant number 17501), which provided free samples during the study period without interfering with the study results.

Conflict of Interest

There is a financial conflict of interest with the funder Inspire Pharmaceutical Company.

Ethics Approval and Consent to Participate

This study was approved by Alexandria University and was conducted in line with ethical principles. Moreover, the study protocol adheres to the ethical principles outlined in the

1975 Declaration of Helsinki. The trial was retrospectively registered on October 20, 2022; the trial registration serial number is 0305757, and the reference number is FWA NO: 00018699. Each participant's consent was acquired in advance. Patients provided written informed consent before participating in this research.

Consent for Publication

Patients who took part in this study agreed to publish their data.

Availability of Data

The materials supporting the study's results are included in the article. Additional information is accessible through the following link: https://drive.google.com/drive/folders/1m9wImunKzTJIV5H8zx1D3-_PYh1KsJ4L?usp=sharing

References

[1] Wang YK, Kuo FC, Liu CJ, Wu MC, Shih HY, Wang SS, *et al*. Diagnosis of *Helicobacter pylori* infection: Current options and developments. World J Gastroenterol 2015;21:11221-35.
doi: 10.3748/wjg.v21.i40.11221

[2] Malfertheiner P, Megraud F, Rokkas T, Gisbert JP, Liou JM, Schulz C, *et al*. Management of *Helicobacter pylori* infection: The maastricht VI/florence consensus report. Gut 2022;71:1724-62.
doi: 10.1136/gutjnl-2022-327745

[3] Nordestgaard MA, Spiegelhauer RM, Frandsen HT, Gren C, Stauning AT, Andersen PL. Clinical manifestations of the Epsilonproteobacteria (*Helicobacter pylori*). In: Roesler BM, editor. *Helicobacter Pylori*. London: IntechOpen; 2018. p. 21-32.
doi: 10.5772/intechopen.80331

[4] Liou JM, Malfertheiner P, Lee Y, Sheu B, Sugano K, Cheng H, *et al*. Screening and eradication of *Helicobacter pylori* for gastric cancer prevention: The Taipei global consensus. Gut 2020;69:2093-112.
doi: 10.1136/gutjnl-2020-322368

[5] Chey WD, Leontiadis GI, Howden CW, Moss SF. ACG clinical guideline: Treatment of *Helicobacter pylori* infection. Am J Gastroenterol 2017;112(2):212-39.
doi: 10.1038/ajg.2016.563

[6] Malfertheiner P, Megraud F, O'Morain CA, Atherton J, Axon AT, Bazzoli F, *et al*. Management of *Helicobacter pylori* infection--the maastricht IV/ florence consensus report. Gut 2012;61:646-64.
doi: 10.1136/gutjnl-2012-302084

[7] Sachs G, Meyer-Rosberg K, Scott DR, Melchers K. Acid, protons and *Helicobacter pylori*. Yale J Biol Med 1996;69:301-16.

[8] Sugimoto M, Furuta T, Shirai N, Kodaira C, Nishino M, Ikuma M, *et al*. Evidence that the degree and duration of acid suppression are related to *Helicobacter pylori* eradication by triple therapy. Helicobacter 2007;12:317-23.
doi: 10.1111/j.1523-5378.2007.00508.x

[9] Graham DY, Fischbach L. *Helicobacter pylori* treatment in the era of increasing antibiotic resistance. Gut 2010;59(8):1143-53.
doi: 10.1136/gut.2009.192757

[10] Smith SM, O'Morain C, McNamara D. Antimicrobial susceptibility testing for Helicobacter pylori in times of increasing antibiotic resistance. World J Gastroenterol 2014;20:9912-21.
doi: 10.3748/wjg.v20.i29.9912

[11] Alboraie M, Elhossary W, Aly OA, Abbas B, Abdelsalam L, Ghaith D, *et al*. Egyptian recommendations for management of *Helicobacter pylori* infection: 2018 report. Arab J Gastroenterol 2019;20:175-9.
doi: 10.1016/j.ajg.2019.09.001

[12] Metwally M, Ragab R, Abdel Hamid HS, Emara N, Elkholy H. *Helicobacterpylori* antibiotic resistance in Egypt: A single-center study. Infect Drug Resist 2022;15:5905-13.
doi: 10.2147/IDR.S386082

[13] Murakami K, Furuta T, Ando T, Nakajima T, Inui Y, Oshima T, *et al*. Multi-center randomized controlled study to establish the standard third-line regimen for *Helicobacter pylori* eradication in Japan. J Gastroenterol 2013;48:1128-35.
doi: 10.1007/s00535-012-0731-8

[14] Shin JM, Inatomi N, Munson K, Strugatsky D, Tokhtaeva E, Vagin O, *et al*. Characterization of a novel potassium-competitive acid blocker of the gastric H, K-ATPase, 1-[5-(2-fluorophenyl)-1-(pyridin-3-ylsulfonyl)-1H-pyrrol-3-yl]-N-methylmethanamine monofumarate (TAK-438). J Pharmacol Exp Ther 2011;339:412-20.
doi: 10.1124/jpet.111.185314

[15] Hori Y, Imanishi A, Matsukawa J, Tsukimi Y, Nishida H, Arikawa Y, *et al*. 1-[5-(2-fluorophenyl)-1-(pyridin-3-ylsulfonyl)-1H-pyrrol-3-yl]-N-methylmethanamine monofumarate (TAK-438), a novel and potent potassium-competitive acid blocker for the treatment of acid-related diseases. J Pharmacol Exp Ther 2010;335:231-8.
doi: 10.1124/jpet.110.170274

[16] Scott D, Weeks D, Melchers K, Sachs G. The life and death of *Helicobacter pylori*. Gut 1998;43 Suppl 1:S56-60.
doi: 10.1136/gut.43.2008.s56

[17] Hunt RH, Scarpignato C. Potassium-competitive acid blockers (P-CABs): Are they finally ready for prime time in acid-related disease? Clin Transl Gastroenterol 2015;6:e119.
doi: 10.1038/ctg.2015.39

[18] Scarpignato C, Hunt RH. Acid suppressant therapy: A step forward with potassium-competitive acid blockers. Curr Treat Options Gastroenterol 2021;19:94-132.
doi: 10.1007/s11938-020-00330-x

[19] Graham DY, Lu H, Shiotani A. Vonoprazan-containing *Helicobacter pylori* triple therapies contribution to global antimicrobial resistance. J Gastroenterol Hepatol 2021;36:1159-63.
doi: 10.1111/jgh.15252

[20] Matsukawa J, Hori Y, Nishida H, Kajino M, Inatomi N. A comparative study on the modes of action of TAK-438, a novel potassium-competitive acid blocker, and lansoprazole in primary cultured rabbit gastric glands. Biochem Pharmacol 2011;81:1145-51.
doi: 10.1016/j.bcp.2011.02.009

[21] Hori Y, Matsukawa J, Takeuchi T, Nishida H, Kajino M, Inatomi N. A study comparing the antisecretory effect of TAK-438, a novel potassium-competitive acid blocker, with lansoprazole in animals. J Pharmacol Exp Ther 2011;337:797-804.
doi: 10.1124/jpet.111.179556

[22] Sakurai Y, Nishimura A, Kennedy G, Hibberd M, Jenkins R, Okamoto H, *et al*. Safety, tolerability, pharmacokinetics, and pharmacodynamics of single rising TAK-438 (Vonoprazan) doses in healthy male Japanese/non-Japanese subjects. Clin Transl Gastroenterol 2015;6:e94.
doi: 10.1038/ctg.2015.18

[23] Jenkins H, Sakurai Y, Nishimura A, Okamoto H, Hibberd M, Jenkins R, *et al*. Randomised clinical trial: Safety, tolerability, pharmacokinetics and pharmacodynamics of repeated doses of TAK-438 (vonoprazan), a novel potassium-competitive acid blocker, in healthy male subjects. Aliment Pharmacol Ther 2015;41:636-48.
doi: 10.1111/apt.13121

[24] Murakami K, Sakurai Y, Shiino M, Funao N, Nishimura A, Asaka M. Vonoprazan, a novel potassium-competitive acid blocker, as a component of first-line and second-line triple therapy for *Helicobacter pylori* eradication: A phase III, randomised, double-blind study. Gut 2016;65:1439-46.
doi: 10.1136/gutjnl-2015-311304

[25] Malfertheiner P, Bazzoli F, Delchier JC, Celiński K, Giguère M, Rivière M, *et al*. *Helicobacter pylori* eradication with a capsule containing bismuth subcitrate potassium, metronidazole, and tetracycline given with omeprazole versus clarithromycin-based triple therapy: A randomised, open-label, non-inferiority, phase 3 trial. Lancet 2011;377:905-13.
doi: 10.1016/S0140-6736(11)60020-2

[26] Muralidharan K. On sample size determination. Math J Interdiscip Sci 2014;3:55-64.
doi: 10.15415/mjis.2014.31005

[27] Fallone CA, Chiba N, Van Zanten SV, Fischbach L, Gisbert JP, Hunt RH, *et al*. The toronto consensus for the treatment of *Helicobacter pylori* infection in adults. Gastroenterology 2016;151:51-69.
doi: 10.1053/j.gastro.2016.04.006

[28] Malfertheiner P, Megraud F, O'Morain CA, Gisbert JP, Kuipers E, Axon A, *et al*. Management of *Helicobacter pylori* infection-the Maastricht V/florence consensus report. Gut 2017;66:6-30.
doi: 10.1136/gutjnl-2016-312288

[29] Kim BJ, Yang CH, Song HJ, Jeon SW, Kim GH, Kim HS, *et al*. Online registry for nationwide database of *Helicobacter pylori* eradication in Korea: Correlation of antibiotic use density with eradication success. Helicobacter 2019;24:e12646.
doi: 10.1111/hel.12646

[30] Liou JM, Fang YJ, Chen CC, Bair MJ, Chang CY, Lee YC, *et al*. Concomitant, bismuth quadruple, and 14-day triple therapy in the first-line treatment of *Helicobacter pylori*: A multicentre, open-label, randomised trial. Lancet 2016;388:2355-65.
doi: 10.1016/S0140-6736(16)31409-X

[31] Fiorini G, Zullo A, Saracino IM, Gatta L, Pavoni M, Vaira D. Pylera and sequential therapy for first-line *Helicobacter pylori* eradication: A culture-based study in real clinical practice. Eur J Gastroenterol Hepatol 2018;30:621-5.
doi: 10.1097/MEG.0000000000001102

[32] McNicholl AG, Marin AC, Molina-Infante J, Castro M, Barrio J, Ducons J, *et al*. Randomised clinical trial comparing sequential and concomitant therapies for *Helicobacter pylori* eradication in routine clinical practice. Gut 2014;63(2):244-9.
doi: 10.1136/gutjnl-2013-304820

[33] Ozaki H, Harada S, Takeuchi T, Kawaguchi S, Takahashi Y, Kojima Y, *et al*. Vonoprazan, a novel potassium-competitive acid blocker, should be used for the *Helicobacter pylori* eradication therapy as first choice: A large sample study of vonoprazan in real world compared with our randomized control trial using second-generation proton pump inhibitors for *Helicobacter pylori* eradication therapy. Digestion 2018;97(3):212-8.
doi: 10.1159/000485097

[34] Sakurai Y, Mori Y, Okamoto H, Nishimura A, Komura E, Araki T, *et al*. Acid-inhibitory effects of vonoprazan 20 mg compared with esomeprazole 20 mg or rabeprazole 10 mg in healthy adult male subjects--a randomised open-label cross-over study. Aliment Pharmacol Ther 2015;42:719-30.
doi: 10.1111/apt.13325

[35] Savoldi A, Carrara E, Graham DY, Conti M, Tacconelli E. Prevalence of antibiotic resistance in *Helicobacter*

pylori: A systematic review and meta-analysis in world health organization regions. Gastroenterology 2018;155:1372-82.
doi: 10.1053/j.gastro.2018.07.007

[36] Villoria A, Garcia P, Calvet X, Gisbert JP, Vergara M. Meta-analysis: High-dose proton pump inhibitors vs. standard dose in triple therapy for *Helicobacter pylori* eradication. Aliment Pharmacol Ther 2008;28:868-77.
doi: 10.1111/j.1365-2036.2008.03807.x

[37] Mégraud F, Graham DY, Howden CW, Trevino E, Weissfeld A, Hunt B, *et al*. Rates of antimicrobial resistance in *Helicobacter pylori* isolates from clinical trial patients across the US and Europe. Am J Gastroenterol 2023;118:269-75.
doi: 10.14309/ajg.0000000000002045

[38] Lyu QJ, Pu QH, Zhong XF, Zhang J. Efficacy and safety of vonoprazan-based versus proton pump inhibitor-based triple therapy for *Helicobacter pylori* eradication: A meta-analysis of randomized clinical trials. Biomed Res Int 2019;2019:9781212.
doi: 10.1155/2019/9781212

[39] Mahrous NL, Nasrelden E, Hassan M, Aboelmagd M. Efficacy of Vonoprazan-based triple therapy for cure of *H. Pylori* infection among patients attending GIT outpatient clinic at Suez Canal university hospital. Microbes Infect Dis 2023;4:506-13.
doi: 10.21608/mid.2023.191490.1459

[40] Furuta T, Yamade M, Kagami T, Uotani T, Suzuki T, Higuchi T, *et al*. Dual therapy with vonoprazan and amoxicillin is as effective as triple therapy with Vonoprazan, amoxicillin and clarithromycin for eradication of *Helicobacter pylori*. Digestion 2020;101:743-51.
doi: 10.1159/000502287

DOI: http://doi.org/10.36922/jctr.24.00043

Journal of Clinical and Translational Research 2024; 10(6): 325-333

Journal of Clinical and Translational Research

Journal homepage: http://www.jctres.com/en/home

ORIGINAL ARTICLE

Establishment and characterization of patient-derived high-grade glioma cell lines, and validation of their tumorigenicity in murine xenograft model

Natália Barreto[1], Valquiria Aparecida Matheus[1], Ingrid Mayara Cavalcante Trevisan[1], Thaís Tuasca Jareño[2], Giovanna Marques Antunes[2], Julio Cesar de Moraes[3], Liana Verinaud[4]*, Jean Gonçalves de Oliveira[2], José Carlos Esteves Veiga[2], João Luiz Vitorino-Araujo[2], Catarina Rapôso[1]*

[1]Faculty of Pharmaceutic Sciences, University of Campinas, Campinas, São Paulo, Brazil, [2]Division of Neurosurgery, Department of Surgery, Santa Casa de São Paulo School of Medical Sciences, São Paulo, Brazil, [3]Imunocel Laboratory, Campinas, São Paulo, Brazil, [4]Department of Structural and Functional Biology, Biology Institute, University of Campinas, Campinas, São Paulo, Brazil

ARTICLE INFO

Article history:
Received: June 14, 2024
Accepted: October 8, 2024
Published Online: December 5, 2024

Keywords:
High-grade gliomas
Cancer cell lines
Human primary cell line
Glioblastoma
Tumorigenicity

**Corresponding authors:*
Catarina Rapôso
Faculty of Pharmaceutic Sciences, University of Campinas, Campinas, São Paulo, Brazil.
Email: raposo@unicamp.br
Liana Verinaud
Department of Structural and Functional Biology, Biology Institute, UNICAMP, Campinas, São Paulo, Brazil.
Email: verinaud@unicamp.br

ABSTRACT

Background: Diffuse high-grade gliomas (HGGs) include the most aggressive types of brain tumors. Despite current treatment options, which include a combination of surgery, radiotherapy, and chemotherapy, the prognosis remains catastrophic. Patients diagnosed with glioblastoma (GB), the most aggressive HGG, have a median survival of <2 years. Cancer cell lines represent an essential tool in cancer research. Once established, these cells can be used to investigate tumor biology and conduct drug screening trials, contributing to the development of new therapeutic options for patients with glioma.
Aim: The aim of the study was to establish and characterize three new HGG cell lines obtained from different patients and validate their tumorigenicity in a murine xenograft model.
Methods: The three tissue samples were immunohistochemically and molecularly classified as astrocytoma IDH-mutant, Grade 3 (C03); GB IDH-wildtype, grade 4 (N07); and astrocytoma IDH-mutant, Grade 3 (L09). These were cultured until the tenth passage for culture establishment. Cell morphology was accessed by light microscopy and phalloidin labeling. To characterize the cell lines, GFAP labeling was performed. Xenograft murine models were used to investigate whether the cell lines retained their tumor-forming ability. Cells from murine tumors were recultured, and morphological evaluation was performed by histopathological analysis.
Results: The three HGG lines were successfully established, and GFAP positivity confirmed their astrocytic origin. Morphologically, the cells presented a fusiform or polygonal shape, with accelerated growth throughout the passages. All three cell lines developed tumors after induction of the xenograft model, and the subculture of these tumors revealed a morphology similar to that of the three cell lines before implantation. Histopathological analysis of the xenograft tumors confirmed the disordered tissue formation commonly found in diffuse gliomas.
Conclusion: The successful establishment of these cell lines and the creation of a biobank will facilitate studies in drug development and glioma tumorigenesis.
Relevance for Patients: The established cell lines will be utilized in assays to analyze glioma tumorigenesis and in screening for novel drug candidates, contributing to the development of new treatments for these patients.

1. Introduction

Diffuse high-grade gliomas (HGGs) are a heterogeneous group of tumors that originate from glial or glial precursor cells and are among the most aggressive and prevalent

DOI: http://doi.org/10.36922/jctr.24.00028

brain tumors in adults [1]. According to the 2021 World Health Organization (WHO) Classification of Tumors of the Central Nervous System (WHO CNS5), adult diffuse gliomas are classified into: (i) Astrocytoma, IDH-mutant (grades 2, 3, or 4), (ii) oligodendroglioma, IDH-mutant, and 1p/19q-codeleted (grades 2 or 3); and (iii) glioblastoma (GB), IDH-wildtype (grade 4) [2]. CNS WHO Grades 1 – 4 are related to the degree of malignancy, with a higher grade corresponding to a poorer prognosis [2-4]. Standard treatments for HGGs involve a combination of maximal surgical resection, radiotherapy, and chemotherapy [5,6]. However, these treatments have limited efficacy in preventing glioma progression. GB is the most common and highly malignant type of brain tumor in adults, with a median survival of <2 years for most patients [7,8]. Given the poor outcomes associated with HGGs, there is a need to explore new therapeutic approaches or even improve the efficacy of conventional therapies against these tumors.

Patient-derived cancer cell lines are the most commonly used models to study tumor biology and discover novel therapeutics, not only *in vitro* but also in murine *in vivo* assays [9,10]. Once established, malignant cell cultures provide excellent and permanent materials for studying tumor biology and behavior. They facilitate the analysis of bioactive components produced by tumors, the determination of cell viability and proliferation, and the assessment of cell migration and invasion under treatment conditions [11]. Therefore, *in vitro* assays are a fundamental step in drug development, as they permit screening for agents that selectively target tumors. For example, the successful establishment of a human GB cell line (named NG97) [11,12] allowed our research group to identify spider venom molecules with antitumor effects [3,13-16]. These studies emphasize the importance of establishing cancer cell lines. However, their focus primarily remained on one glioma cell type (GB-NG97). Considering the heterogeneity of gliomas, trials involving multiple cell types from different patients could provide a more comprehensive understanding of the effects of animal venom molecules on these tumors.

Despite being an excellent model for cancer research and drug development, establishing cell lines from fresh tissue obtained from patients is time-consuming and challenging. In contrast to established cell lines, primary cells are sensitive to new environments and more susceptible to contamination. Bian *et al.* [17] reported that the success rate of cell line establishment from fresh tumor tissues is around 10%. In the present study, we aimed to establish and characterize three new human cell lines derived from fresh tissue samples of three male patients diagnosed with HGGs. Through a simple yet carefully optimized process, we aimed to establish the cell lines after only a few passages, ensuring they became stable while remaining as close as possible to the original tumor tissue. These newly established cell lines will facilitate future studies related to the understanding of glioma biology, especially due to their distinct histological and molecular characteristics. These cell lines will also enable our research group to conduct new tests investigating the effects of animal venom molecules. A well-established tumor cell bank provides heterogeneous cell lines and opens perspectives for studies aimed at developing new treatments against these tumors.

2. Methods

2.1. Ethical considerations

Tissue samples were obtained from the department of neurosurgery and imaging examinations were acquired from the department of radiology, both at the Central Hospital of Santa Casa (Brazil) after informed patient consent (Termo de Consentimento Livre e Esclarecido [TCLE]). Tumor samples were acquired following the ethical guidelines of the Research Ethics Committee of the University of Campinas (UNICAMP, Brazil; CAAE: 15215219.5.0000.5404) and the Central Hospital of Santa Casa (Brazil; CAAE: 15215219.5.3001.5479). Animal experiments were performed in accordance with the Ethical Principles in Animal Research, adopted by the Brazilian College of Animal Experimentation (Colégio Brasileiro de Experimentação Animal [COBEA]); all procedures were previously approved by the Animal Use Ethics Committee (CEUA/UNICAMP; 6200-1/2023). The animals were carefully monitored and cared for daily to ensure their well-being. They were kept in standard filter-top cages with unrestricted access to sterile water and food in the Animal Facility of the Institute of Biology, Department of Functional and Structural Biology (UNICAMP).

2.2. Specimen collection

After surgical resection, tissue samples were obtained from three different patients: a 55-year-old male (specimen designated C03), a 56-year-old male (N07), and a 36-year-old male (L09). Under aseptic conditions, a portion of the samples from each patient was placed in separate falcon tubes containing Iscove's Modified Dulbecco´s Medium (IMDM; #l7633; Sigma-Aldrich, United States of America [USA]) supplemented with 10% fetal bovine serum (FBS) and penicillin-streptomycin-amphotericin B solution (10.000 U/mL; #A5955; Sigma-Aldrich, USA) (pH 7.4) (referred to as complete medium). These samples were intended for the preparation of primary cell cultures. The remaining portions were placed in other falcon tubes containing 10% formaldehyde and sent to a histopathology laboratory, where the tumors were characterized immunohistochemically and molecularly according to WHO CNS5 2021, as follows: astrocytoma IDH-mutant, WHO Grade 3 (C03); GB IDH-wildtype, WHO grade 4 (N07); and astrocytoma IDH-mutant, WHO Grade 3 (L09).

2.3. Cell lines establishment

Tumor specimens were maintained in a complete medium, minced into 1 – 2 mm^3 fragments, and centrifuged (1500 rpm, 4°C, 5 min) to remove debris. The supernatant was then discarded, and the cells (pellet) were seeded into 25 cm^2 culture bottles. Primary cells were cultured (IMDM) and maintained at 37°C in a 5% CO_2 humidified atmosphere until they reached the tenth passage. Each passage involves releasing the cells from the bottle using a cell scraper and transferring them to a larger bottle or two other bottles. By the tenth passage, the cells were observed to be stable after thawing, indicating successful

DOI: http://doi.org/10.36922/jctr.24.00028

establishment. Large quantities of the three cell lines were then routinely frozen at −80°C in FBS supplemented with 10% (v/v) dimethyl sulfoxide (DMSO; #D2650; Sigma-Aldrich, USA) and stored long-term in a cryogenic freezer within liquid nitrogen vapor (biobank). For the immunofluorescence assay, cells were thawed, cultured, and allowed to reach 90% confluence before being carefully scraped into 48-well plates (Corning Costar®, USA). In addition, 3×10^5 cells were also obtained for the tumorigenicity assay as described below.

2.4. Immunofluorescence

Characterization and authentication of the three established cell lines were assessed using immunostaining for glial fibrillary acidic protein (GFAP), an astrocyte marker. Cell morphology was also assessed using phalloidin to selectively label actin filaments. This assay was based on a standardized protocol in our laboratory, which was described in a previous study [13]. Cells were initially seeded in 48-well plates (2×10^5 cells/well) with a complete medium. At 90% confluence, the medium was removed from the wells and replaced with fresh medium. Cells were then fixed with 4% paraformaldehyde (PFA) (15 min), washed three times with phosphate-buffered saline (PBS) (pH 7.4), and incubated with a permeabilization solution (0.1% Triton X-100 in PBS) for 10 min at room temperature. After, the wells were washed with PBS and then treated with a blocking solution (1% bovine serum albumin [BSA] 467 supplemented 0.2% Tween 20 in PBS) for 1 h. Subsequently, the cells were incubated with a Phalloidin probe (1:200, P5282; Sigma-Aldrich, USA) diluted in 0.3% BSA solution (supplemented with 0.1% Tween 20 in PBS) for 2 h at room temperature. Following this, the wells were washed with PBS and incubated overnight with anti-GFAP (1:500; #16825-I-AP; Proteintech, USA) in the same dilution solution. A negative control group without anti-GFAP incubation was also prepared. The next day, cells were washed again with PBS and incubated with rhodamine (TRITC) – conjugated goat anti-rabbit IgG (1:100; #SA00007-2; Proteintech, USA) for 1 h, and then counterstained with a drop of the nucleus dye DAPI (#P36971; ThermoFisher, USA). Cell imaging was performed using Apotome.2 (Zeiss, Germany) and analyzed with Zen 2.6 and Image J software.

2.5. Tumorigenicity in RAG$^{-/-}$ black mice

To investigate tumorigenicity, 3×10^5 cells from each of the three cell lines were suspended in 0.1 mL PBS and injected subcutaneously into the dorsal flank of adult immunodeficient C57BL/6 RAG$^{-/-}$ female or male mice (12 months old). The animals were monitored weekly during tumor development. After 22 days of cell implantation, the mice were anesthetized with ketamine (80 mg/kg) and xylazine (10 mg/kg) and euthanized. Tumors were excised and divided into two parts for different processing methods. One part was fixed in 4% PFA and embedded in paraffin for tissue analysis by hematoxylin and eosin (H&E) staining. The other part was placed in a falcon tube containing a complete medium for subculture, morphological analysis, and creation of a biobank.

2.6. Tumor histopathology

Tumor pieces designated for tissue analysis were immersed in PFA for 24 h. Thereafter, the tissue pieces were washed with distilled water 3 times (10 min each) to remove any residual PFA. The samples were then dehydrated through an ethanol gradient and embedded in Paraplast (#P3558; Sigma-Aldrich, USA). Sections of 5 µm were obtained and stained with H&E before evaluation under a microscope.

2.7. Morphological evaluation

For evaluation of morphology, the three established cell lines (obtained from patients) and those acquired after tumor excision from mice were seeded in 6-well plates (2×10^5 cells/well) and incubated at 37°C, 5% CO_2 for 48 h. The cells were then photographed under an inverted microscope (Nikon Eclipse Ts2; Nikon, Japan) and the NIS-Elements D software to analyze their general morphology. The entire methodology used in this work is summarized and exemplified in Figures 1A and B.

3. Results

3.1. Establishment and biobanking of the three high-grade glioma cell lines from patient tumor tissues and morphological evaluation

A tumor mass was observed in the MRI of the patient before surgery (Figures 2A, 3A, and 4A). Using *in vitro* patient-derived specimens, the three HGG cell lines (C03, N07, and L09) were successfully established. From the primary culture, it was possible to freeze, thaw, and subculture cells, allowing the creation of a biobank and the performance of *in vitro* characterization (GFAP labeling), as described below. During the first 2 weeks of culture, the GB (N07) cell line grew faster than the astrocytoma (C03 and L09) cell lines. Later, growth was similar for all three HGG cell lines. All of them reached the tenth passage in about 2 months. Under light microscopy, all three cell lines grew in monolayer and most of them exhibited spindle-shaped and polygonal morphologies; some of them exhibited long protrusions (Figures 2B, 3B, and 4B).

3.2. Tumorigenicity of the three high-grade glioma cell lines in C57BL/6 RAG$^{-/-}$ mice and morphological evaluation

To assess whether the three cell lines retained their tumor-forming ability, a tumorigenicity assay was conducted. *In vivo,* xenograft tumors were developed after subcutaneous implantation of all three established cell lines (Figures 2C and D; 3C and D; and 4C; and D). After 22 days of inoculation, the animals were anesthetized and the tumor masses were excised. The tumors reached a volume of 2.5, 0.7, and 2.02 cm^3, with weights of 1.6, 0.8, and 1.5 g, respectively (for C03, N07, and L09). The morphology of the xenograft tumors during subculture resembled the cell line characteristics of the three cell lines before implantation, displaying spindle-shaped and polygonal morphologies (Figures 2E, 3E, and 4E).

DOI: http://doi.org/10.36922/jctr.24.00028

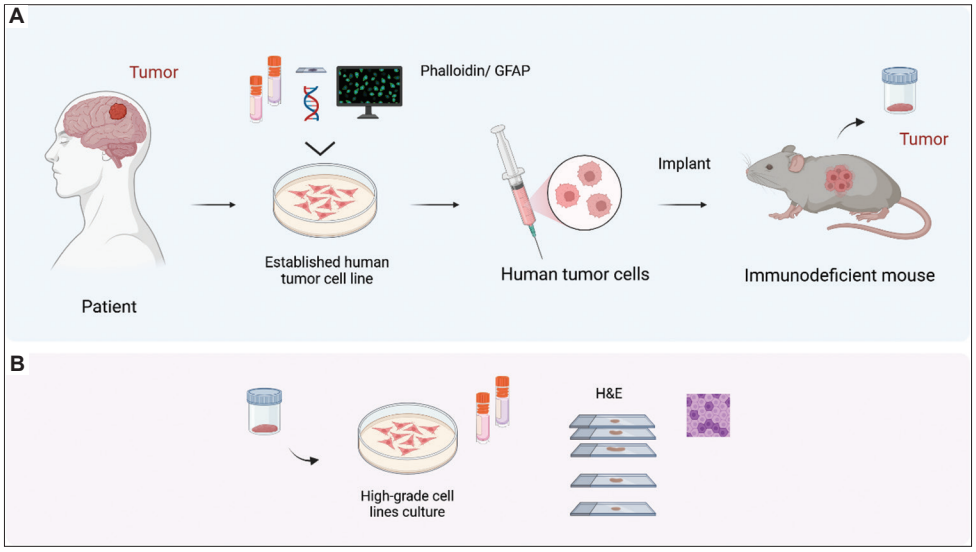

Figure 1. Methodology summary. Establishment of patient-derived high-grade glioma cell lines (C03, N07, and L09), and *in vivo* tumorigenicity analysis. (A) After patient consent, portions of the obtained tumor samples were cultured until they reached the tenth passage (establishment). Large amounts of these cells were frozen to create a biobank. Morphological analysis and characterization of the cell lines (GFAP labeling) were performed using an inverted microscope and immunofluorescence assays, respectively. The remaining tumor portions were destined for histopathological and molecular classification. Subsequently, the cell lines were implanted in a xenogeneic murine model to evaluate their tumor-forming capacity. (B) Fragments of the tumors developed and excised from the animals were sub-cultivated for their establishment and for creating another biobank. Other tumor fragments were processed for histopathological evaluation (H&E staining). GFAP: Glial fibrillary acidic protein; H&E: Hematoxylin and eosin. The figure was created in BioRender; Santos, N. (2023; https://BioRender.com/w44p823)

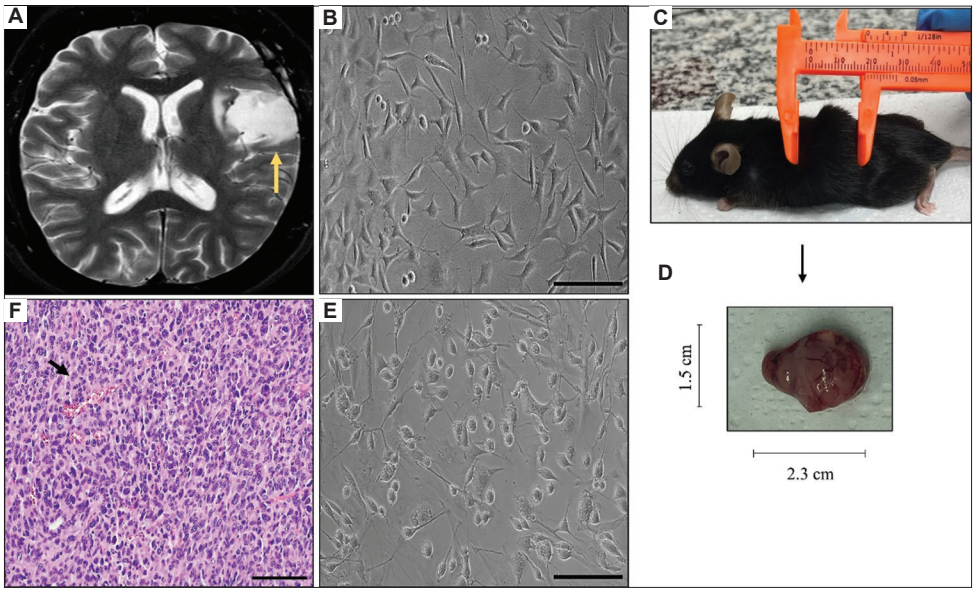

Figure 2. Astrocytoma IDH-mutant, grade 3 (C03) human cells. (A) MRI of the patient before surgery; the tumor mass is indicated with a yellow arrow. (B) C03 cell line during its culture and establishment. The cell line was observed under an inverted microscope after the tenth passage, exhibiting spindle-shaped and polygonal morphologies; some exhibiting long protrusions. (C) Tumorigenicity test of C03 in C57BL/6 $RAG^{-/-}$ mice. (D) The solid tumor obtained (volume: 2.5 cm^3; weight: 1.6 g). (E) C03 cell line during its culture after excision of the animal's tumor. Note that their morphology resembles that of the C03 cell line before implantation. (F) Histopathology (H&E) of the subcutaneous tumor, displaying increased cellularity, variation in nuclear size, and mitotic figures (black arrow). Scale bars: 100 µm (B and E); 50 µm (F)
Abbreviations: MRI: Magnetic resonance imaging; H&E: Hematoxylin and eosin

3.3. Histopathology of tumor mass

Histopathological examination was performed to assess whether the xenografted tumors retained features observed in astrocytic tumors. Tumors originating from all three cell lines indicated increased cellularity, variation in nuclear size, and mitotic figures, similar to astrocytic tumors (Figures 2F, 3F, and 4F).

DOI: http://doi.org/10.36922/jctr.24.00028

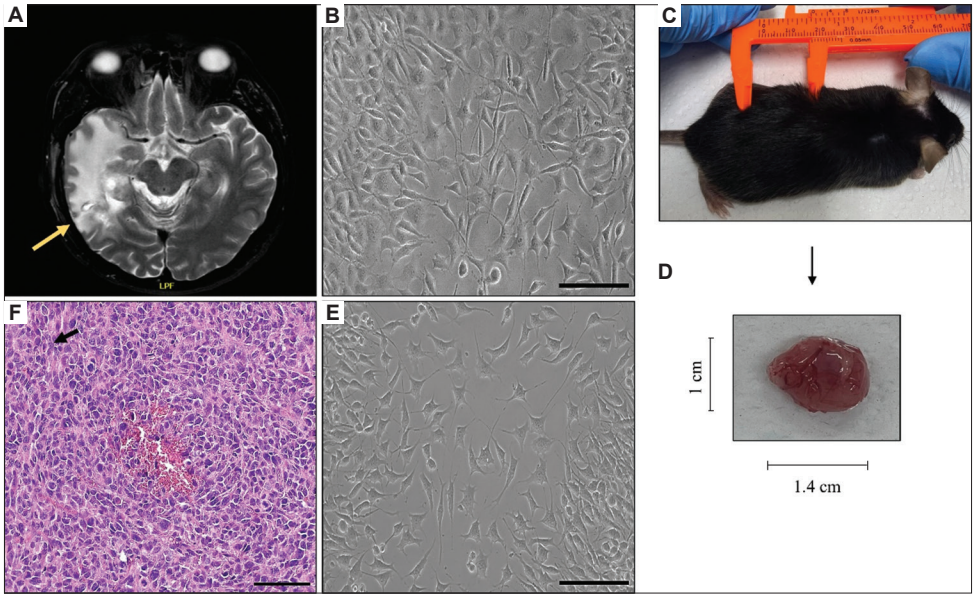

Figure 3. Glioblastoma IDH-wildtype, Grade 4 (N07) human cells. (A) MRI of the patient before surgery; the tumor mass is indicated with a yellow arrow. (B) N07 cell line during its culture and establishment. The cell line was observed under an inverted microscope after the tenth passage, exhibiting spindle-shaped and polygonal morphologies; some exhibiting long protrusions. (C) Tumorigenicity test of N07 in C57BL/6 $RAG^{-/-}$ mice. (D) The solid tumor obtained (volume: 0.7 cm^3; weight: 0.8 g). (E) N07 cell line during its culture after excision of the animal's tumor. Note that their morphology resembles that of the N07 cell line before implantation. (F) Histopathology (H&E) of the subcutaneous tumor, displaying increased cellularity, variation in nuclear size, and mitotic figures (black arrow). Scale bars: 100 µm (B and E); 50 µm (F)
Abbreviations: MRI: Magnetic resonance imaging; H&E: Hematoxylin and eosin

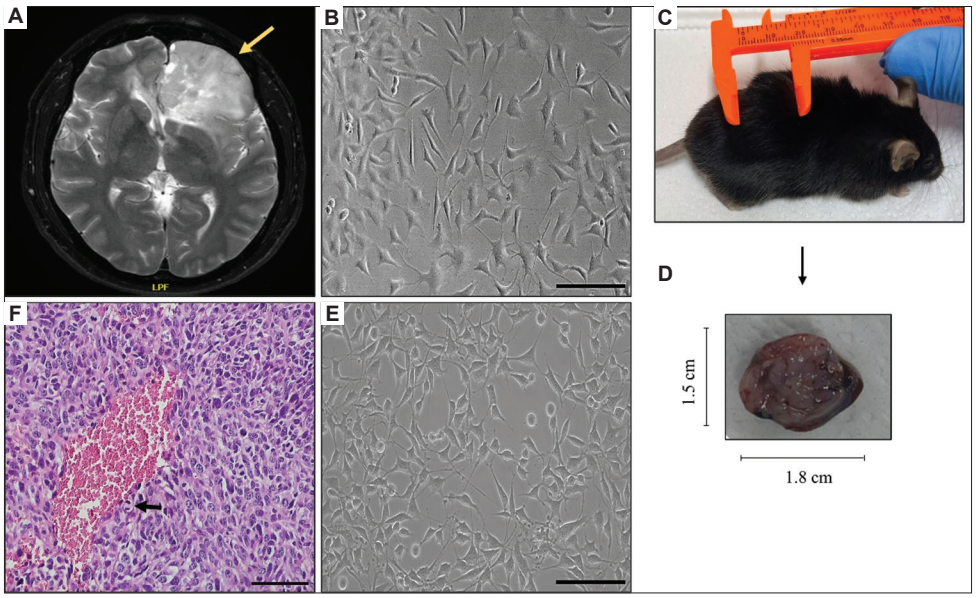

Figure 4. Astrocytoma IDH-mutant, Grade 3 (L09) human cells. (A) MRI of the patient before surgery; the tumor mass is indicated with a yellow arrow. (B) L09 cell line during its culture and establishment. The cell line was observed under an inverted microscope after the tenth passage, exhibiting spindle-shaped and polygonal morphologies; some exhibiting long protrusions. (C) Tumorigenicity test of L09 in C57BL/6 $RAG^{-/-}$ mice. (D) The solid tumor obtained (volume: 2.02 cm^3; weight: 1.5 g). (E) L09 cell line during its culture after excision of the animal's tumor. Note that their morphology resembles that of the L09 cell line before implantation. (F) Histopathology (H&E) of the subcutaneous tumor, displaying increased cellularity, variation in nuclear size, and mitotic figures (black arrow). Scale bars: 100 µm (B and E); 50 µm (F)
Abbreviations: MRI: Magnetic resonance imaging; H&E: Hematoxylin and eosin

3.4. Phalloidin and GFAP labeling

To characterize and authenticate the three established cell lines, immunostaining for GFAP, a reliable marker of astrocytic cells, was performed. Immunofluorescence was also carried out to evaluate glioma cell morphology by phalloidin labeling. All three HGG cells displayed a rounded morphology with some thin extensions. GFAP labeling was positive in all HGGs, confirming their astrocytic origin (Figures 5A-D, 6A-D, and 7A-D).

DOI: http://doi.org/10.36922/jctr.24.00028

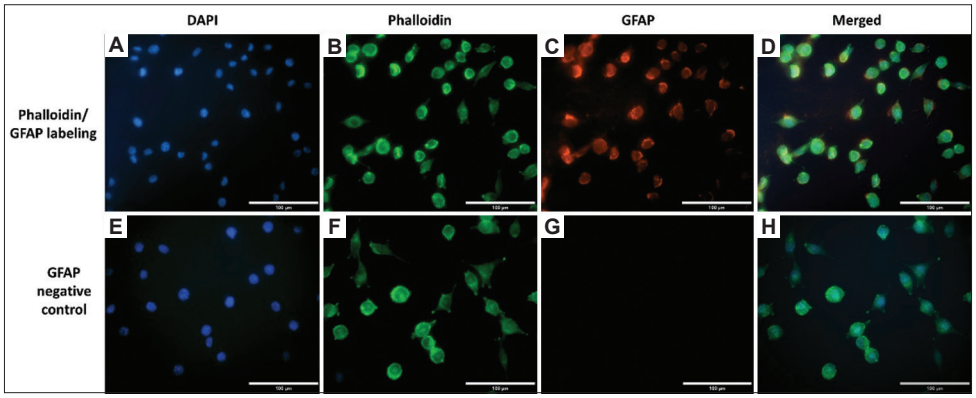

Figure 5. Astrocytoma IDH-mutant, Grade 3 (C03) human cells. (A-D) Phalloidin probe and GFAP labeling. The cells displayed rounded morphology with some thin extensions; GFAP staining was positive in C03 cells, confirming astrocytic origin. (E-H) Negative control (without GFAP labeling). Scale bars: 100 μm

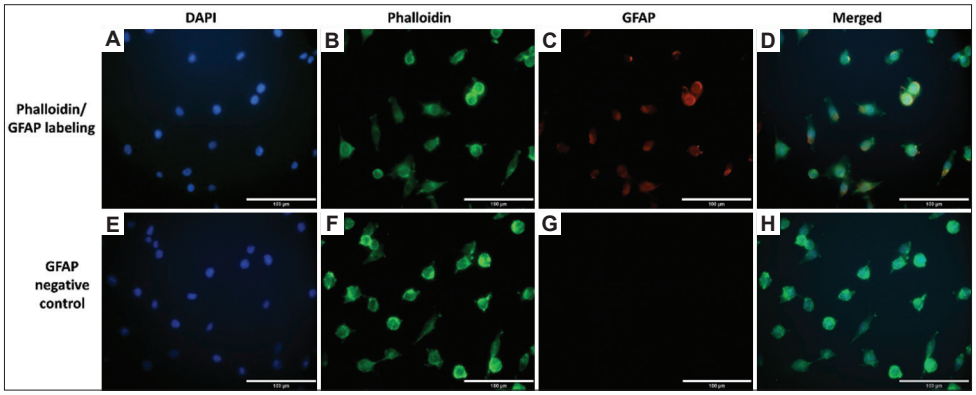

Figure 6. Glioblastoma IDH-wildtype, Grade 3 (N07) human cells. (A-D) Phalloidin probe and GFAP labeling. The cells displayed rounded morphology with some thin extensions; GFAP staining was positive in N07 cells, confirming astrocytic origin. (A-H) Negative control (without GFAP labeling). Scale bars: 100 μm

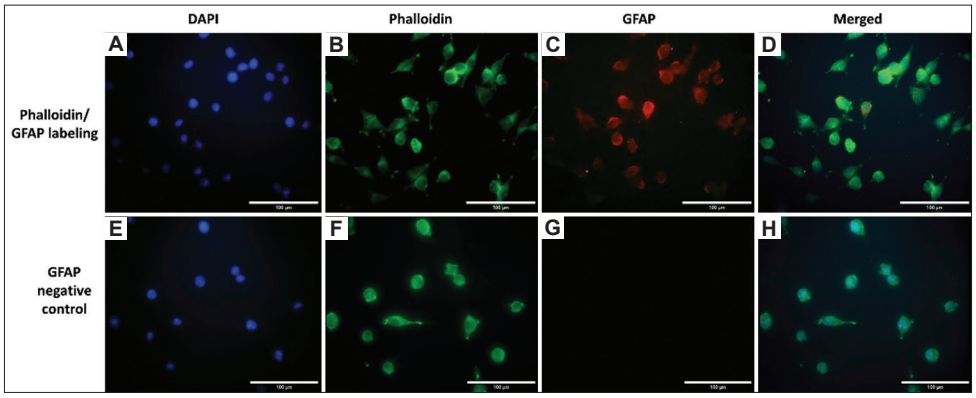

Figure 7. Astrocytoma IDH-mutant, grade 3 (L09) human cells. (A-D) Phalloidin probe and GFAP labeling. The cells displayed rounded morphology with some thin extensions; GFAP staining was positive in L09 cells, confirming astrocytic origin. (E-H) Negative control (without GFAP labeling). Scale bars: 100 μm

Negative controls (without GFAP labeling) were also performed (Figures 5E-H, 6E-H, and 7E-H).

4. Discussion

Cancer cell lines are one of the most powerful tools in cancer research. Establishing new primary cancer cell lines obtained directly from patient tumor tissue is essential to understanding tumor behavior and biology, as well as establishing a preclinical model for testing and developing new drugs [10,18]. These cell lines are commonly used to assess drug sensitivity, resistance, and toxicity. However, after numerous passages, these cell lines can accumulate genetic and epigenetic changes that may

DOI: http://doi.org/10.36922/jctr.24.00028

hinder many preclinical studies from translating into clinical applications. The occurrence of multiple passages makes these cell lines less similar to the original tissue [19,20]. This allows newly established cell lines to become a better study model than commercially available cell lines. In the present study, we were able to establish three new HGG cell lines (C03, N07, and L09) after 10 passages, obtained directly from primary tumors of different patients. During the adaptation period, astrocytoma cell lines (C03 and L09) slowly adhered to the culture flasks and began to proliferate more rapidly until reaching the tenth passage. Interestingly, the GB cell line (N07) grew faster in the first 2 weeks of culture than the astrocytomas. Thereafter, growth was similar for all three HGG cell lines. These differences may be related to GB being a more aggressive tumor; however, after the 2nd week, its growth remained similar to that of the other cell lines. After reaching the tenth passage (approximately 2 months), it was noted that they became stable after thawing.

Compared to other cell culture models, like sphere culture, adherent cells are easy to manipulate and are ideal for drug screening experiments, such as cell proliferation, viability, and migration assays. Although easy to manipulate, primary cultures are more susceptible to contamination. They are also more sensitive to microenvironmental components, making the choice of an appropriate culture medium essential. Cheng *et al.* [21] cultured 10 GB cell lines from different patients using high-glucose DMEM + 10% FBS, but only one of them (GWH04) acquired unlimited proliferation capacity. In the present study, all three HGG cell lines acquired stability and high replicative ability with complete medium (IMDM + 10% FBS), without the need for additional glucose supplementation. Morphological analysis is commonly used to assess the characteristics of cancer cell lines. Despite being different types of gliomas, all three HGG cell lines grew in a monolayer and exhibited spindle-shaped and polygonal morphologies. These morphological findings are in agreement with studies of other established primary glioma cell lines. Grube *et al.* [20] established 16 of 34 GB cell lines that exhibited a spindle-form or polygonal-to-amorphous morphology and grew as a monolayer. In the present study, we also investigated cell morphology by labeling cytoskeleton components (using the phalloidin probe). The cells exhibited a morphology similar to those observed by light microscopy. Interestingly, the presence of rounder rather than polygonal cells was noted.

The differences observed in morphology may be related to the time at which the cells were imaged, as phalloidin labeling was performed in the initial weeks of culture, whereas light microscopy was conducted after establishment. Machado *et al.* [11] observed a similar pattern during GB (NG97) establishment: in the first passages, GB cultures grew more slowly and presented a more rounded shape. At the 13th passage, dendritic-like cells, with more extensive cytoplasmatic extensions, appeared in the culture. Subsequently, spindle-shaped cells appeared as the culture became dense. We hypothesize that these differences may be related to the heterogeneity of the tumor and the slow adaptation of the cells to a new environment. Cells may create more connections during culture, forming additional cellular extensions that connect to one another as they adapt to the new environment. Despite the GB (C03) cell line growing faster at the beginning of culture, its morphology remained similar to the other astrocytic (N07 and L09) cell lines. In addition to morphological analyses, to characterize and confirm the established cell lines as astrocytoma and GB, immunofluorescence staining for GFAP was performed. GFAP, a protein involved in the structure and function of the cytoskeleton, is commonly used as a marker of astrocytes [21,22]. Our results indicated that the three HGGs were positive for GFAP, confirming their astrocytic origin. Furthermore, for the validation of the cell lines, it was also important to evaluate whether the cell lines maintained the ability to form tumors. Studies report that the implantation of tumor cell lines in mice does not always lead to tumor development [21]. However, this is an important factor to reliably attest to the tumorigenicity of new tumor cell lines. In the present study, all three HGG cell lines were tumorigenic in RAG-/- C57BL6 mice, indicating that the cells are neoplastic and malignant. Histopathological analysis of xenograft tumors from all three cell lines revealed increased cellularity, variation in nuclear size, and mitotic figures. These characteristics are in line with other studies describing malignant astrocytoma tumors, which are distinguished by high mitotic activity and increased cellularity [23,24]. The difference in size and weight of the tumors obtained did not influence the histopathological analyses, which were very similar, despite being from three different cell lines.

5. Conclusion

Three HGG cell lines (C03, N07, and L09) obtained from different patients were successfully established. Characterization confirmed their astrocytic origin, and validation in a xenograft murine model demonstrated their ability to form tumors post-establishment. Therefore, these newly established cell lines prove to be useful for studying cell and molecular biology, as well as for the development of new glioma treatments.

Acknowledgments

We would like to thank the support and the access to equipment provided by the National Institute of Science and Technology on Photonics Applied to Cell Biology (INFABIC) at the State University of Campinas. Figure 1 was created using BioRender (BioRender.com).

Funding

This study was financed by the São Paulo Research Foundation (FAPESP; #2019/10003-3 [Natália Barreto's scholarship], #2022/03543-4, and #2015/04194-0), the National Council for Scientific and Technological Development (Conselho Nacional de Desenvolvimento Científico e Tecnológico [CNPq]; 148156/2019-3 [Natália Barreto's scholarship]), and the Education, Research, and Extension Support Fund (Fundo de Apoio ao Ensino, à Pesquisa e à Extensão [FAEPEX/UNICAMP]; #2588/20, #2124/21, #2569/21, #2389/22,

#2768/22, #3515/23, and #3462/23). INFABIC is co-funded by FAPESP (#2014/50938-8) and CNPq (#465699/2014-6).

Conflicts of Interest

The authors declare no conflicts of interest.

Ethics Approval and Consent to Participate

All methods and experiments were performed strictly following the guidelines of the Research Ethics Committee from the University of Campinas (UNICAMP - Campinas, São Paulo, Brazil): CAAE: 15215219.5.0000.5404, and from the Central Hospital of Santa Casa (São Paulo, Brazil): CAAE: 15215219.5.3001.5479. Animal experimentation was carried out following the Ethical Principles on Animal Research, adopted by the Brazilian College of Animal Experimentation (Colégio Brasileiro de Experimentação Animal, COBEA), and approved by the Ethics Committee on the Use of Animals (CEUA/UNICAMP; 6200-1/2023). All authors provided consent for publication.

Consent for Publication

Tissue samples were obtained after informed patient consent (Informed Consent Form [TCLE]). By signing the TCLE, patients agreed to disclose images and data for research purposes.

Availability of Data

Data are available from the corresponding author upon reasonable request.

References

[1] Ostrom QT, Cioffi G, Gittleman H, Patil N, Waite K, Kruchko C, *et al*. CBTRUS Statistical Report: Primary Brain and Other Central Nervous System Tumors Diagnosed in the United States in 2012-2016. Neuro Oncol 2019;21:v1-100.
doi: 10.1093/neuonc/noz150

[2] Louis DN, Perry A, Wesseling P, Brat DJ, Cree IA, Figarella-Branger D, *et al*. The 2021 WHO Classification of Tumors of the Central Nervous System: A summary. Neuro Oncol 2021;23:1231-51.
doi: 10.1093/neuonc/noab106

[3] Barreto Dos Santos N, Bonfanti AP, da Rocha-E-Silva TA, Da Silva PI Jr., Da Cruz-Höfling MA, Verinaud L, *et al*. Venom of the *Phoneutria nigriventer* Spider Alters the CELL Cycle, Viability, and Migration of Cancer Cells. J Cell Physiol 2019;234:1398-415.
doi: 10.1002/jcp.26935

[4] Higginbottom SL, Tomaskovic-Crook E, Crook JM. Considerations for Modelling Diffuse High-grade Gliomas and Developing Clinically Relevant Therapies. Cancer Metastasis Rev 2023;42:507-41.
doi: 10.1007/s10555-023-10100-7

[5] Stupp R, Mason WP, van den Bent MJ, Weller M, Fisher B, Taphoorn MJ, *et al*. Radiotherapy Plus Concomitant and Adjuvant Temozolomide for Glioblastoma. N Engl J Med 2005;352:987-96.
doi: 10.1056/NEJMoa043330

[6] Rapôso C, Vitorino-Araujo JL, Barreto N. Molecular Markers of Gliomas to Predict Treatment and Prognosis: Current State and Future Directions. In: Brain Tumor Center of Excellence, Wake Forest Baptist Medical Center Comprehensive Cancer Center, Winston Salem, NC, USA, Debinski W, editors. Gliomas. Australia: Exon Publications; 2021. p. 171-86.
doi: 10.36255/exonpublications.gliomas.2021.chapter10

[7] Ostrom QT, Gittleman H, Farah P, Ondracek A, Chen Y, Wolinsky Y, *et al*. CBTRUS Statistical Report: Primary Brain and Central Nervous System Tumors Diagnosed in the United States in 2006-2010. Neuro Oncol 2013;15:ii1-56.
doi: 10.1093/neuonc/not151

[8] Tan AC, Ashley DM, López GY, Malinzak M, Friedman HS, Khasraw M. Management of Glioblastoma: State of the Art and Future Directions. CA Cancer J Clin 2020;70:299-312.
doi: 10.3322/caac.21613

[9] Barretina J, Caponigro G, Stransky N, Venkatesan K, Margolin AA, Kim S, *et al*. The Cancer Cell Line Encyclopedia Enables Predictive Modelling of Anticancer Drug Sensitivity. Nature 2012;483(7391):603-7.
doi: 10.1038/nature11003

[10] Huo KG, D'Arcangelo E, Tsao MS. Patient-derived Cell Line, Xenograft and Organoid Models in Lung Cancer Therapy. Transl Lung Cancer Res 2020;9:2214-32.
doi: 10.21037/tlcr-20-154

[11] Machado CM, Schenka A, Vassallo J, Tamashiro WM, Gonçalves EM, Genari SC, *et al*. Morphological Characterization of a Human Glioma Cell Line. Cancer Cell Int 2005;5:13.
doi: 10.1186/1475-2867-5-13

[12] Grippo MC, Penteado PF, Carelli EF, Cruz-Höfling MA, Verinaud L. Establishment and Partial Characterization of a Continuous Human Malignant Glioma Cell Line: NG97. Cell Mol Neurobiol 2001;21:421-8.
doi: 10.1023/a:1012662423863

[13] Barreto N, Caballero M, Bonfanti AP, de Mato FC, Munhoz J, da Rocha-E-Silva TA, *et al*. Spider Venom Components Decrease Glioblastoma Cell Migration and Invasion through RhoA-ROCK and Na+/K+-ATPase β2: Potential Molecular Entities to Treat Invasive Brain Cancer. Cancer Cell Int 2020;20:576.
doi: 10.1186/s12935-020-01643-8

[14] Bonfanti AP, Barreto N, Munhoz J, Caballero M, Cordeiro G, Rocha-E-Silva T, *et al*. Spider Venom Administration Impairs Glioblastoma Growth and

Modulates Immune Response in a Non-clinical Model. Sci Rep 2020;10:5876.
doi: 10.1038/s41598-020-62620-9

[15] Caballero M, Barreto N, Bonfanti AP, Munhoz J, Rocha-E-Silva T, Sutti R, *et al*. Isolated Components From Spider Venom Targeting Human Glioblastoma Cells and Its Potential Combined Therapy With Rapamycin. Front Mol Biosci 2022;9:752668.
doi: 10.3389/fmolb.2022.752668

[16] De Mato FC, Barreto N, Cordeiro G, Munhoz J, Bonfanti AP, Da Rocha-E-Silva TA, *et al*. Isolated Peptide from Spider Venom Modulates Dendritic Cells *In Vitro*: A Possible Application in Oncoimmunotherapy for Glioblastoma. Cells 2023;12:1023.
doi: 10.3390/cells12071023

[17] Bian X, Cao F, Wang X, Hou Y, Zhao H, Liu Y. Establishment and Characterization of a New Human Colon Cancer Cell Line, PUMC-CRC1. Sci Rep 2021;11:13122.
doi: 10.1038/s41598-021-92491-7

[18] Feng F, Huang C, Xiao M, Wang H, Gao Q, Chen Z, *et al*. Establishment and Characterization of Patient-derived Primary Cell Lines as Preclinical Models for Gallbladder Carcinoma. Transl Cancer Res 2020;9:1698-710.
doi: 10.21037/tcr.2020.02.04

[19] Gillet JP, Calcagno AM, Varma S, Marino M, Green LJ, Vora MI, *et al*. Redefining the Relevance of Established Cancer Cell Lines to the Study of Mechanisms of Clinical Anti-cancer Drug Resistance. Proc Natl Acad Sci U S A 2011;108:18708-13.
doi: 10.1073/pnas.1111840108

[20] Grube S, Freitag D, Kalff R, Ewald C, Walter J. Characterization of Adherent Primary Cell Lines From Fresh Human Glioblastoma Tissue, Defining Glial Fibrillary Acidic Protein as a Reliable Marker in Establishment of Glioblastoma Cell Culture. Cancer Rep Hoboken 2021;4:e1324.
doi: 10.1002/cnr2.1324

[21] Cheng F, Wan X, Wang B, Li Y, Peng P, Xu S, *et al*. Establishment and Characteristics of GWH04, A New Primary Human Glioblastoma Cell Line. Int J Oncol 2022;61:139.
doi: 10.3892/ijo.2022.5429

[22] Brenner M, Messing A. Regulation of GFAP Expression. ASN Neuro 2021;13:1-32.
doi: 10.1177/1759091420981206

[23] Wood MD, Halfpenny AM, Moore SR. Applications of Molecular Neuro-oncology - A Review of Diffuse Glioma Integrated Diagnosis and Emerging Molecular Entities. Diagn Pathol 2019;14:29.
doi: 10.1186/s13000-019-0802-8

[24] Ferris SP, Hofmann JW, Solomon DA, Perry A. Characterization of Gliomas: From Morphology to Molecules. Virchows Arch 2017;471:257-69.
doi: 10.1007/s00428-017-2181-4

DOI: http://doi.org/10.36922/jctr.24.00028

Journal of Clinical and Translational Research 2024; 10(6): 334-342

Journal of Clinical and Translational Research

Journal homepage: http://www.jctres.com/en/home

ORIGINAL ARTICLE

Impact of non-invasive ventilation immediately after extubation on clinical and functional outcomes in patients submitted to coronary artery bypass grafting: a clinical trial

André Luiz Lisboa Cordeiro[1]*, Carolina Moura Silva[1], Kênia de Jesus Lima[1], Mayana Rocha de Santana[1], André Raimundo França Guimarães[2], Patrícia Forestieri[3], Luiz Alberto Forgiarini Júnior[4]

[1]Department of Physiotherapy, Nobre University Center, Feira de Santana, Bahia, Brazil, [2]Noble Institute of Cardiology, Feira de Santana, Bahia, Brazil, [3]Department of Cardiology and Cardiovascular Surgery, Sao Paulo Hospital, Federal University of Sao Paulo, São Paulo, Brazil, [4]Department of Medicine and Physiotherapy, Catholic University of Pelotas, Porto Alegre, Rio Grande do Sul, Brazil

ARTICLE INFO

Article history:
Received: March 3, 2024
Accepted: November 15, 2024
Published Online: December 5, 2024

Keywords:
Myocardial revascularization
Extubation
Non-invasive ventilation

**Corresponding author:*
André Luiz Lisboa Cordeiro
Department of Physiotherapy, Nobre University Center, 2116 - Centro, Feira de Santana, Bahia, 44001-008, Brazil.
Email: andre.cordeiro@grupponobre.net

ABSTRACT

Background: The use of non-invasive ventilation (NIV) after coronary artery bypass grafting (CABG) may help reduce loss of functional capacity and complications in patients. However, the evidence regarding its immediate versus conventional use is controversial.
Aim: The aim of the study was to assess the impact of immediate NIV after extubation on oxygenation and the functional capacity of patients undergoing CABG.
Methods: This study was a randomized clinical trial involving patients of both sexes, aged 18 years or older, who have undergone elective CABG with median sternotomy and cardiopulmonary bypass. Patients were assessed before and after surgery using the Functional Independence Measure (FIM), 6-min walk test (6MWT), and the Medical Research Council (MRC) scale for peripheral muscle strength. On the 1st day after the surgery, two groups were formed: immediate NIV (NIVI) and conventional NIV (NIVC). Hemogasometry was performed before and after NIV, and complication rates were assessed. NIVI was administered 1 h after orotracheal extubation, while NIVC was performed on the first post-operative day, 24 h after extubation. After discharge, the above variables were re-evaluated.
Results: A total of 79 patients were evaluated; 46 (58.22%) were men, with a mean age of 65 ± 9 years. NIVI reduced the reintubation rate in one patient (3%) compared to NIVC with five patients (12%) ($p = 0.01$). In the post-intervention period, the inspired oxygen fraction (F_IO_2) was 0.43 ± 0.07 in the NIVC group and 0.30 ± 0.10 in the NIVI group ($p = 0.01$). The post-intervention PaO_2/F_IO_2 ratio was 191 ± 45 in the NIVC group and 266 ± 29 in the NIVI group ($p < 0.001$); the ratio one day later was 210 ± 39 in the NIVC group and 279 ± 37 in the NIVI group ($p < 0.001$). From the 6MWT, the INVI group reported a reduction of 51 ± 36 m compared to a reduction of 95 ± 40 m in the NIVC group ($p < 0.01$).
Conclusion: NIVI after extubation of patients undergoing CABG reduced the loss of functional capacity, improved blood gas levels, and decreased the rate of reintubation.
Relevance for Patients: This study suggests that the use of NIVI after extubation in patients undergoing CABG may improve recovery, preserve lung function, and reduce complications such as reintubation.

1. Introduction

Cardiac surgery (CS) is a widely utilized treatment due to the high incidence of cardiovascular diseases worldwide [1]. Among the most common procedures, coronary artery bypass grafting (CABG) stands out as a method that improves blood flow in patients

DOI: http://doi.org/10.36922/jctr.24.00011

with symptomatic myocardial ischemia, particularly when one or more coronary arteries are obstructed by atheromatous plaques [2]. Although patients undergoing CABG often display significant results, most of them would develop post-operative pulmonary disorders [3].

Approximately 30% of patients undergoing heart surgery experience a decrease in muscle strength and lung function after the procedure [4]. Consequently, the emergence of pulmonary complications can lead to unfavorable clinical outcomes, such as atelectasis, pneumonia, pulmonary edema, and acute respiratory failure, negatively impacting functional recovery [5,6]. Several factors, including age, overweight, sex, type of surgery, and intraoperative conditions, can contribute to the development of these complications [7].

Non-invasive ventilation (NIV) can be employed immediately after extubation to minimize pulmonary dysfunction, reduce the length of stay in the intensive care unit (ICU), and enhance the functional capacity of these patients [8-11]. According to the Brazilian mechanical ventilation (MV) guideline, NIV should be performed immediately after extubation. However, in some institutions, it is typically implemented on the first post-operative day per the institution's protocol [12]. There is still limited evidence regarding the validation of clinical and functional outcomes when comparing NIV administered immediately after extubation to that performed on the first post-operative day.

Therefore, this study aims to demonstrate the impact of administering NIV at different times on patients undergoing CABG [12]. While many ICU services routinely use NIV on the first post-operative day, we hypothesize that its use immediately after extubation may increase the likelihood of favorable outcomes. The purpose of this study was to compare the clinical and functional impact of two post-extubation (or prophylactic) non-invasive MV protocols for patients undergoing CABG surgery.

2. Methods

2.1. Study design

This was a randomized controlled clinical trial conducted with patients admitted to the ICU at the Noble Institute of Cardiology (Instituto Nobre de Cardiologia; INCARDIO) in Feira de Santana, Brazil, from January 2016 to October 2019. The study was approved by the Research Ethics Committee of Noble College (Faculdade Nobre) in Feira de Santana, Brazil (approval number: 1,405,821). All patients were informed about the study's objectives and provided written informed consent. The trial was registered in the Brazilian Registry of Clinical Trials (ReBEC; trial number RBR-9wkvm5b).

2.2. Eligibility criteria

This study included patients of both sexes, aged 18 years or older, who underwent elective CABG with median sternotomy and cardiopulmonary bypass. Patients with hemodynamic instability (mean arterial pressure lower than 60 mmHg) before NIV, those who were uncooperative, or those with contraindications for NIV were excluded. In addition, patients with chronic pulmonary disease, physical limitations that compromised functional testing (such as amputations), difficulty understanding the test instructions, the need for surgical reintervention, more than 24 h on invasive MV, and those who refused to sign the consent form were also excluded. The eligibility criteria were assessed by a researcher specifically assigned to this task.

2.3. Outcomes

The primary outcome was oxygenation and functional capacity. Secondary outcomes included the impact on functional variables, such as the Functional Independence Measure (FIM), peripheral muscle strength, pulmonary complications, mortality, and length of stay in the ICU and hospital. The primary oxygenation outcome was assessed before, immediately after, and one day following the application of NIV. Functional capacity was evaluated preoperatively and on the day of hospital discharge. Likewise, secondary outcomes were also assessed preoperatively and on the day of hospital discharge.

2.4. Study protocol

In the pre-operative phase, all patients underwent functional assessment using FIM, a 6-min walk test (6MWT), and the Medical Research Council (MRC) scale for peripheral muscle strength.

The following day, patients were taken to the operating room, where the surgery was performed by the same surgical team using median sternotomy and cardiopulmonary bypass, employing grafts from the internal thoracic artery or bypass. All patients left the operating room with subxiphoid and intercostal drains and were transferred to the ICU with full analgesia. Anesthetic agents included induction with midazolam, propofol, or etomidate; analgesia with fentanyl and/or morphine; neuromuscular blockade with rocuronium, vecuronium, or cisatracurium; and maintenance with isoflurane, transitioning to an infusion of propofol or dexmedetomidine before transport to the ICU. Intubation was performed using a 7.5- or 8.0-mm internal diameter endotracheal tube. Physiotherapists typically employed a pressure-controlled volume-guaranteed ventilation mode throughout the study, targeting normocapnia or mild hypocapnia while avoiding hypoxemia. Default ventilator settings included a tidal volume (VT) of 500 mL and positive end-expiratory pressure (PEEP) of 0 cm H_2O. All patients received pain relief with 1 g paracetamol four times daily as needed after discharge. On arrival in the ICU, they were managed according to routine procedures, without any influence from the researchers. Following established weaning criteria, patients were guided toward extubation, after which low-flow oxygen support was initiated to maintain saturation levels at 94 – 97%.

At the hospital where the research was conducted, NIV is routinely performed on the first post-operative day. Shortly after extubation, eligible patients were randomized using an electronic system (http://randomizer.org/form.htm) by a professional not part of the research team, ensuring the confidentiality of

DOI: http://doi.org/10.36922/jctr.24.00011

the procedure. Sealed, opaque, and sequentially numbered envelopes were used to conceal the allocation sequence until interventions were assigned. Researchers responsible for evaluations were blinded to the intervention and control groups.

Patients were divided into two groups: The immediate NIV group (NIVI) and the conventional NIV group (NIVC). The NIVI group received NIV immediately following orotracheal extubation, while the NIVC group received NIV on the first post-operative day, approximately 24 h after extubation.

NIV was administered using the Servo-S ventilator (Dräger Medical, Germany) in pressure support ventilation mode, with pressure sufficient to maintain tidal volume between 6 to 8 mL/kg, PEEP starting at 5 cm H_2O and increasing to 12 cm H_2O, and an inspired oxygen fraction (F_IO_2) of 30%. A face mask was utilized, and PEEP adjustments were protocol-driven for all patients. This therapy was maintained for 40 min in both groups and was performed only once. Arterial blood gas analysis was conducted before and after NIV for evaluation of gas exchange, with a follow-up analysis performed one day later for assessment of oxygenation.

On the day of discharge from the ICU, patients were reassessed using FIM and the MRC scale, and they were also evaluated for pulmonary complications, mortality, and length of stay in the ICU. These assessments were repeated on the day of hospital discharge, along with a repetition of the 6MWT. All patients received standard physiotherapy assistance, which included kinesiotherapy, cycle ergometry, and walking exercises.

Outcomes related to post-operative complications were assessed by a blinded radiologist. Gasometric and functional evaluations were conducted by a blinded physician and physiotherapist, respectively. Due to the nature of the intervention, blinding of patients and unit staff was not feasible.

2.5. Measurements

The 6MWT was conducted following the recommendations of the American Thoracic Society (ATS) in a flat, obstacle-free corridor measuring 30 m [13]. Before the test, patients were given a rest period of at least 10 min. During this time, contraindications were assessed, and vital signs were recorded, including blood pressure (using a Premium Aneroid Sphygmomanometer [Welch Allyn, United States of America [USA] and Littmann 3M® stethoscope [USA]), pulse oximetry (pulse oximeter from Rossmax® [USA]), dyspnea level (assessed using the Borg scale), heart rate (measured by palpating the radial artery for 1 min), and respiratory rate (evaluated by observing respiratory movements over 1 min).

Patients were instructed to walk as quickly as possible – without running – around the corridor for 6 min. Encouragement was provided at intervals throughout the test. At the end of the 6 min, the examiner recorded the total distance covered.

Throughout the entire protocol, patients were monitored closely. The test would be interrupted if there was an increase in systolic or diastolic blood pressure greater than 30% from baseline, a heart rate drop of more than 20% from baseline, peripheral oxygen saturation below 90%, or a respiratory rate exceeding 30 breaths/min.

The FIM aims to assess what a person can actually achieve, regardless of diagnosis, generating a valid score for functional limitations. This scale evaluates the patient's ability to perform self-care, maintain sphincter control, transfer, and ambulate, as well as cognitive functions such as communication and memory. Scores range from 1 to 7, with the lowest score indicating total dependence and the highest score reflecting complete independence from a functional perspective. The maximum possible score is 126 points when all variables are combined [14].

The MRC scale evaluates peripheral muscle strength by assessing the ability to overcome resistance in six muscle groups: shoulder abductors, elbow flexors, wrist extensors, hip flexors, knee extensors, and ankle dorsiflexors. Each group is scored bilaterally from 0 to 5, where 0 indicates the absence of contraction and five represents the patient overcoming maximum resistance imposed by the examiner. The minimum score for this test is 0 (indicative of quadriplegia), while the maximum score is 60 (indicating preserved muscle strength). A score below 48 may suggest the presence of polyneuromyopathy [15].

2.6. Measurement of pulmonary function

To assess vital capacity (VC), the Ferraris Mark 8 Wright Respirometer (Wright, USA) was used. The respirometer was unlocked and cleared; a facial mask was then placed on the individual's face. The patient was instructed to take a deep breath until reaching total lung capacity, followed by a slow and gradual expiration until reaching residual volume. After this, the respirometer was locked, and the result was recorded. The test was repeated three times, with the highest value being considered.

Peak expiratory flow was measured using the Mini Wright® peak flow meter (Wright, USA). During the evaluation, the patient was seated with the head in a neutral position and a nasal clip to prevent air escape through the nostrils. The patient took a deep breath to total lung capacity, followed by a forced expiration into the device. After three measurements, the highest value was selected, ensuring that no individual measurement differed by more than 40 L from the others.

2.7. Calculation of statistical power

In our study, 79 patients were evaluated, revealing a standard deviation in average oxygenation of 191 mmHg in the control group and 266 mmHg in the training group, resulting in a difference of 75 mmHg between the two groups.

The convenience sample provided a statistical power of 30% (alpha = 5%). A convenience sample is a non-random sampling method where participants are selected based on their easy availability or proximity to the researcher, rather than through a random or systematic process. This sample type is often used in exploratory research, where time, cost, or access to a specific population is limited. However, as it is not random, a convenience sample may not be representative of the broader population, potentially introducing bias into the results.

In addition, the standard deviation in average distance walked was 322 m in the control group and 378 m in the training group,

DOI: http://doi.org/10.36922/jctr.24.00011

with a difference of 56 m between the groups. This sample allowed for a statistical power of 10% (alpha = 5%).

2.8. Statistical analysis

Data analysis was conducted using the Statistical Package for the Social Sciences (SPSS) version 20.0 (IBM, USA). Normality was assessed using the Shapiro–Wilk test. Categorical variables were analyzed using the Chi-square test, while continuous data were expressed as the mean ± standard deviation. To evaluate oxygenation, functional capacity, and length of stay – both intra- and intergroup – paired Student's *t*-test and independent *t*-test were employed, respectively. Pulmonary complications and mortality were assessed using the Chi-square test. A *p*-value of < 0.05 was considered statistically significant.

3. Results

During the study period, 101 patients were admitted for CS. Of these, 22 were excluded for the following reasons: three required surgical reintervention before extubation, 10 remained on MV for more than 24 h, five refused to participate in the study, two died before extubation, and two patients could not provide blood gas data before NIV (Figure 1). Consequently, 79 patients were included in the study, with no loss to follow-up after randomization; 42 were allocated to the NIVC group, and 37 to the NIVI group.

Table 1 presents the clinical and surgical characteristics of the patients. Among them, the male gender was predominant, comprising 46 patients (58.22%), with a mean age of 65 ± 9 years. Arterial hypertension was the most prevalent comorbidity. The other variables are detailed in Table 1.

Significant differences were observed in F_IO_2 and the PaO_2/F_IO_2 ratio. Post-intervention, the F_IO_2 in the NIVC and NIVI groups were 0.43 ± 0.07 and 0.30 ± 0.10, respectively ($p = 0.01$). One day later, the F_IO_2 for the NIVC group was 0.40 ± 0.09, compared to 0.30 ± 0.05 in the NIVI group ($p = 0.04$). The PaO_2/F_IO_2 ratio in the NIVI group was significantly higher at 75 (95% confidence interval [CI]: 45 – 91) immediately after NIV and 69 (95%CI: 33 to 82) one day later. Additional values are presented in Table 2.

Table 3 displays the functional outcomes between the studied groups at various time points during the research. The FIM and MRC scores did not display statistically significant variation when comparing the groups at pre-operative assessment and hospital discharge. However, a significant reduction was noted when analyzing pre-operative scores compared to ICU discharge. The NIVI group demonstrated better performance on 6MWT, with a mean distance loss of 51 ± 36 m, compared to the NIVC group, which experienced a loss of 95 ± 40 m ($p < 0.01$). The difference between the groups in the 6MWT was 44 m (95%CI: 25 to 59).

Regarding post-surgical pulmonary complications, Table 4 presents the results between the groups. The only statistically significant variables were reintubation and pleural effusion, with five NIVC patients versus one NIVI patient for reintubation ($p = 0.01$).

Table 5 illustrates the pulmonary function results, displaying no significant differences between the studied groups.

4. Discussion

NIV performed immediately after extubation has proven to be an effective resource in reducing the loss of functional capacity,

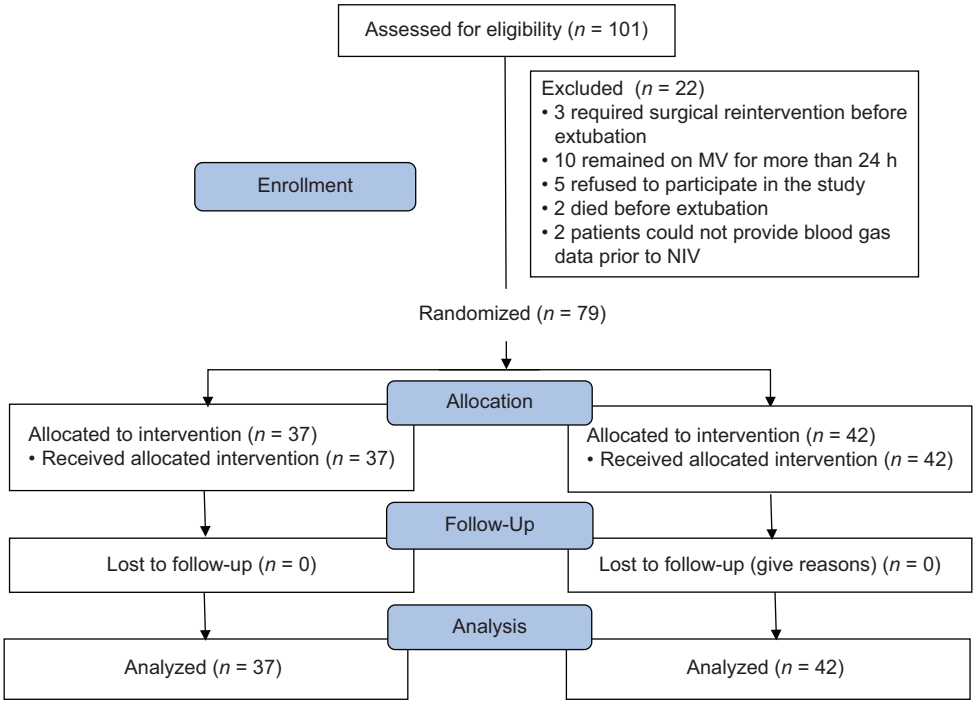

Figure 1. Flowchart related to patient participation in the study
Abbreviation: MV: Mechanical ventilation

DOI: http://doi.org/10.36922/jctr.24.00011

Table 1. Clinical and surgical characteristics of patients randomized according to the NIV groups

Variable	NIV group		*p*
	Conventional (*n*=42)	Immediate (*n*=37)	
Gender			0.52[a]
Male	25 (60%)	21 (57%)	
Female	17 (40%)	16 (43%)	
Age (years)	66±8	64±9	0.36[b]
BMI (kg/m²)	25±3	27±4	0.14[b]
Comorbidities			
SAH	28 (67%)	22 (59%)	0.31[a]
DLP	24 (57%)	17 (46%)	0.21[a]
Diabetes	19 (45%)	14 (38%)	0.54[a]
AMI	5 (12%)	3 (8%)	0.75[a]
Sedentary lifestyle	11 (26%)	9 (24%)	0.69[a]
Surgery time (min)	237±88	244±87	0.23[b]
CPB time (min)	88±21	92±25	0.18[b]
Aortic clamping time (min)	77±18	72±21	0.35[b]
MV time (h)	7±2	8±3	0.76[b]
LVEF (%)	58±6	59±5	0.59[b]

Note: [a]*p*-value obtained from Chi-square test; [b]*p*-value obtained from independent Student's *t*-test. Abbreviations: BMI: Body mass index; SAH: Systemic arterial hypertension; DLP: Dyslipidemia; AMI: Acute myocardial infarction; CPB: Extracorporeal circulation; MV: Mechanical ventilation; LVEF: Left ventricular ejection fraction; NIV: Non-invasive ventilation.

decreasing the rate of reintubation, improving oxygenation up to one day following its use, and shortening hospital stays for patients undergoing CABG. Through this study, we were able to achieve our objective and demonstrate that NIV after extubation has an impact on clinical and functional outcomes. Therefore, hospital services may adopt this type of intervention as a routine practice for this patient profile.

In our study, NIVI patients presented a reduction in the loss of functional capacity, as evidenced by the distance covered in the 6MWT, similar to the findings by Araújo-Filho *et al*. [16] involving patients in the post-operative period of valve replacement. This reduction may be due to the meta-reflex. The realization of NIV increases pulmonary capacity and oxygenation, thus attenuating the metaboreflex, which improves the perfusion of peripheral muscles and leads to an increase in functional performance [17-19].

Performing the 6MWT raises the patient's metabolic rate, requiring greater blood flow to the peripheral muscles. The muscle fibers recruited during the 6MWT are primarily Type I fibers, which rely on oxygen. Therefore, when lung function improves and blood flow rich in oxygen is enhanced, the functional capacity of these patients is significantly better. In the present study, the difference in 6MWT was 44 m between the NIVC and NIVI groups. Gremeaux *et al*. [20] reported that a difference of at least 25 m is clinically important for this patient profile.

Table 2. Blood gas analysis of patients randomized according to the NIV groups

Variable	NIV group		Difference between groups (95%CI)	*p*
	Conventional (*n*=42)	Immediate (*n*=37)		
F_IO_2				
Pre-intervention	0.45±0.11	0.49±0.09	0.04 (−0.1 to 0.2)	0.67
Post-intervention	0.43±0.7	0.30±0.10	0.13 (0.05 to 0.22)	0.01
One day later	0.40±0.09	0.30±0.05	0.1 (0.03 to 0.3)	0.04
PaO_2 (mmHg)				
Pre-intervention	91±15	90±14	1 (−3 to 4)	0.76
Post-intervention	82±12	80±16	2 (−4 to 5)	0.68
One day later	84±11	81±14	3 (−7 to 8)	0.67
PaO_2/F_IO_2				
Pre-intervention	202±34	183±48	19 (−11 to 28)	0.12
Post-intervention	191±45	266±29	75 (45 to 91)	< 0.001
One day later	210±39	279±37	69 (33 to 82)	< 0.001
$PaCO_2$ (mmHg)				
Pre-intervention	37±5	39±4	2 (−4 to 5)	0.78
Post-intervention	41±6	42±3	1 (−4 to 3)	0.87
One day later	40±4	40±2	0 (−2 to 2)	0.91
Tidal volume (mL)				
Pre-intervention	367±22	359±25	8 (−2.53 to 18.53)	0.53
Post-intervention	392±31	411±29	−19 (−32.51 to −5.49)	0.32
One day later	382±21	399±24	−17 (−27.08 to -6.92)	0.39
RR (rpm)				
Pre-intervention	19±2	18±2	1 (0.10 to 1.90)	0.64
Post-intervention	17±2	15±3	2 (0.87 to 3.13)	0.43
One day later	16±2	15±3	1 (−0.13 to 2.13)	0.72

Note: *P*-value obtained from independent Student's *t*-test.
Abbreviations: CI: Confidence interval; FIO_2: Inspired oxygen fraction; PaO_2: Arterial oxygen pressure; $PaCO_2$: Blood pressure of carbon dioxide; RR: Respiratory rate; NIV: Non-invasive ventilation.

DOI: http://doi.org/10.36922/jctr.24.00011

Table 3. Functional results of patients randomized according to the NIV groups

Variable	NIV group		Difference between groups (95%CI)	p^a
	Conventional (n=42)	Immediate (n=37)		
FIM				
Pre-operative	125±1	125±1	0 (−1 to −1)	0.96
ICU discharge	111±3	115±2	4 (−3 to 9)	0.69
Delta[b]	14±2	10±2	4 (−2 to 8)	0.54
Hospital discharge	121±2	123±2	2 (−4 to 5)	0.84
Delta[c]	4±2	2±1	2 (−5 to 6)	0.45
6MWT (m)				
Pre-operative	417±36	429±43	12 (−15 to 22)	0.74
Hospital discharge	322±45	378±39	56 (35 to 71)	0.03
Delta[b]	95±40	51±36	44 (25 to 59)	< 0.01
MRC scale				
Pre-operative	59±1	58±1	1 (−3 to 4)	0.92
ICU discharge	48±4	50±3	2 (−3 to 4)	0.76
Delta[b]	11±3	8±2	3 (−4 to 8)	0.45
Hospital discharge	53±3	55±2	2 (−4 to 6)	0.79
Deltac	6±2	3±1	3 (−5 to 8)	0.43

Note: [a]p-value obtained from independent Student's t-test; [b]delta value obtained from paired Student's t-test between pre-operative and ICU discharge scores; [c]delta value obtained from paired Student's t-test between pre-operative and hospital discharge scores.
Abbreviations: FIM: Functional Independence Measure; ICU: Intensive care unit; 6MWT: 6-min walk test; MRC: Medical Research Council; CI: Confidence interval; NIV: Non-invasive ventilation.

Table 4. Clinical results of patients randomized according to the NIV groups

Variable	NIV group		p
	Conventional (n=42)	Immediate (n=37)	
Complication			
Pneumothorax	5 (12%)	4 (11%)	0.69[a]
Pleural effusion	22 (53%)	10 (27%)	<0.01[a]
Atelectasis	5 (12%)	4 (11%)	0.68[a]
Severe respiratory discomfort	1 (3%)	1 (3%)	0.87[a]
Reintubation	5 (12%)	1 (3%)	0.01[a]
Infection in the sternal wound	2 (5%)	2 (5%)	0.83[a]
In-hospital death	2 (5%)	0 (0%)	0.21[b]
ICU time (days)	3±1	2±1	0.86[b]
Hospital stay (days)	13±5	9±3	0.04[b]

Note: [a]p-value obtained from Chi-square test; [b]p-value obtained from independent Student's t-test.
Abbreviations: ICU: Intensive care unit; NIV: Non-invasive ventilation.

Another fundamental point in this discussion is that NIV tends to enhance the performance of the left ventricle, optimizing cardiac output and improving tissue perfusion [21], thereby improving the functional capacity of these patients. It is important to understand that the application of NIV immediately after extubation effectively optimizes lung function, but improved performance in the walking test can be achieved with enhanced cardiovascular function and peripheral muscles. However, we note that the latter aspect did not influence the result, as there was no difference in the MRC scores between groups. Hence, further validation should be employed using an echocardiogram or assessing myocardial behavior such as ejection fraction, stroke volume, and ventricular mass.

Shoji *et al*. [22] reported a high rate of reintubation among patients undergoing CS and attributed this to various comorbidities (e.g., hypertension and diabetes mellitus) and complications (e.g., pneumonia and renal dysfunction). Therefore, our study suggests using NIVI as a preventive factor for these complications and to reduce the risk of extubation failure.

According to Wu *et al*., [23] the role of NIV remains controversial, as the rate of reintubation does not present a significant difference; however, some authors have proposed immediate NIV application to avoid complications and reduce hospital stay [24,25]. One possibility for the divergent results is the variation in the duration of NIV application, the selection of patients, and the protocols performed.

According to the Brazilian guideline on MV, the use of NIV is indicated in obese, elderly, and patients with more than one comorbidity [12]. As a result, we realized that the patients in our study were older, overweight, and had two or more comorbidities, with satisfactory results after using immediate NIV, including a reduction in the reintubation rate.

Liu *et al*. [26] demonstrated that the prophylactic use of NIV significantly reduced the rate of post-surgical complications and enhanced gas exchange. The immediate use of NIV significantly reduced the rate of atelectasis in our study. The main effect of positive pressure at the end of expiration during NIV is to reopen collapsed alveoli and keep the lung aerated. This reversal of alveolar collapse tends to improve the ventilation/perfusion ratio, generating an increase in gas exchange, which was found in the present study.

In addition, a higher PaO_2/F_IO_2 ratio was observed in NIVI patients even after 24 h from the intervention. Despite the lack

DOI: http://doi.org/10.36922/jctr.24.00011

Table 5. Analysis of pulmonary function of patients randomized according to the NIV groups

Variable	NIV group		Difference between groups (95%CI)	*p*
	Conventional (*n*=42)	Immediate (*n*=37)		
VC (mL/kg)				
Pre-intervention	61±5	62±6	−1 (−3.46 to 1.46)	0.78
Post-intervention	44±6	45±7	−1 (−3.91 to 1.91)	0.87
One day later	45±5	45±5	0 (−2.24 to 2.24)	0.79
PEF (L/min)				
Pre-intervention	475±67	482±69	−7 (−37.50 to 23.50)	0.69
Post-intervention	333±59	356±55	−23 (−48.67 to 2.67)	0.67
One day later	342±55	360±59	−18 (−43.55 to 7.55)	0.56

Abbreviations: VC: Vital capacity; PEF: Peak expiratory flow; NIV: Non-invasive ventilation.

of significance in arterial oxygen pressure, alveolar recruitment resulted in a reduced need for supplemental oxygen, which was reflected in the improved effectiveness of gas exchange.

Therefore, it was possible to maintain the oxygenation levels of patients for a longer duration with a lower O_2 supply, thereby decreasing the toxicity associated with oxygen use. In line with our results, Landoni *et al*. [17] demonstrated that NIV is a useful tool to decrease respiratory work, reduce atelectasis, prevent respiratory failure, and improve gas exchange.

According to Laizo *et al*. [27], complications related to respiratory function are the main causes of increased length of hospital stay. Since the rate of respiratory complications was low in our study, particularly in the NIVI group, this may justify the reduction in the length of hospital stay. This decrease can contribute to lower hospital costs and as a preventive factor for future complications associated with prolonged hospital stay, such as infections and loss of muscle mass.

Systematic reviews found that immediate NIV did not achieve a significant result in terms of length of stay in the ICU or hospital [17,28]. This can be justified by the patient profiles studied, who had low ejection fractions, hypoactivity, and important deficits in muscle strength associated with heart failure. Contrary to our study, the patients evaluated did not present any hemodynamic instability before NIV, did not need surgical reintervention, and mainly obtained positive results on the functionality scale.

In the literature and clinical practice, the choice of whether to perform NIV on the first day after surgery or immediately after extubation remains controversial. This work is evidence that NIV immediately after extubation generates better clinical and functional results a few hours after surgery. Therefore, performing NIV immediately after extubation in selected patients should be adopted as a routine practice.

One of the limitations of this study is the lack of sample size calculation, which would have helped reduce the error margin and effectively strengthen the conclusion. Other limitations include the absence of a pain assessment scale, such as the Visual Analog Scale (VAS), which could have allowed patients to report the degree of pain at the moment. In addition, the study did not use a blind examiner for variables, such as blood gas analysis. Other limitations are the small sample size and the fact that the study was conducted at only one participating institution.

5. Conclusion

The use of NIV immediately after extubation for patients undergoing CABG demonstrated significantly positive impacts, such as reducing the loss of functional capacity, decreasing the rate of reintubation, and improving blood gas exchange, F_IO_2, and the PaO_2/F_IO_2 ratio.

Acknowledgments

None.

Funding

None.

Conflicts of Interest

The authors declare no conflicts of interest.

Ethics Approval and Consent to Participate

The study was approved by the Research Ethics Committee of Noble College in Feira de Santana, Brazil (approval number: 1,405,821). All patients were informed about the study's objectives and provided written informed consent.

Consent for Publication

All research participants authorized the release of their data through a written and signed document.

Availability of Data

Data are available from the corresponding author on reasonable request.

References

[1] Daltro FMS, De Seixas Rocha M, Oliveira L. Effectiveness of positive expiratory pressure on the vital capacity of patients undergoing myocardial revascularization. Rev Bras Fisioter. 2010;14(S1):450.

[2] Lawton JS, Tamis-Holland JE, Bangalore S, Bates ER, Beckie TM, Bischoff JM, *et al*. 2021 ACC/AHA/SCAI guideline for coronary artery revascularization: Executive summary: A report of the American college of cardiology/American heart association joint committee on clinical

practice guidelines. Circulation 2022;145:e4-e17.
doi: 10.1161/CIR.0000000000001039. Erratum in: Circulation 2022;145:e771.

[3] Renault JA, Costa-Val R, Rossetti MB. Respiratory physiotherapy in the pulmonary dysfunction after cardiac surgery. Rev Bras Cir Cardiovasc 2008;23:562-9.
doi: 10.1590/s0102-76382008000400018 [Article in English, Portuguese].

[4] Smith J, Jones M, Brown L. Muscle strength and pulmonary function decline post-cardiac surgery: A longitudinal study. J Cardiothorac Surg 2019;14:45.

[5] Pieczkoski SM, Margarites AGF, Sbruzzi G. Noninvasive ventilation during immediate postoperative period in cardiac surgery patients: Systematic review and meta-analysis. Braz J Cardiovasc Surg 2017;32:301-311.
doi: 10.21470/1678-9741-2017-0032

[6] Borges DL, Nina VJS, Costa MAG, Baldez TE, Santos NP, Lima IM, *et al*. Effects of different PEEP levels on respiratory mechanics and oxygenation after coronary artery bypass grafting. Braz J Cardiovasc Surg 2013;28:380-385.
doi: 10.5935/1678-9741.20130058

[7] Ferreira LL, Souza NMD, Vitor ALR, Bernardo AFB, Valenti VE, Vanderlei LCM. Ventilação mecânica não-invasiva no pós-operatório de cirurgia cardíaca: Atualização da literatura. Braz J Cardiovasc Surg 2012;27:446-52.
doi: 10.5935/1678-9741.20120074

[8] Esquinas AM, Gill H, Mina B. Postoperative noninvasive ventilation in patients undergoing coronary artery bypass grafting: A small step with great repercussions. J Thorac Cardiovasc Surg 2013;146:1299.
doi: 10.1016/j.jtcvs.2013.06.053

[9] Méndez VMF, Oliveira MF, Baião ADN, Xavier PA, Gun C, Sperandio PA, *et al*. Hemodynamics and tissue oxygenation effects after increased in positive end-expiratory pressure in coronary artery bypass surgery. Arch Physiother 2017;7:2.
doi: 10.1186/s40945-016-0030-4

[10] Esquinas AM, De Santo LS. Noninvasive ventilation after surgical myocardial revascularization for left-ventricular dysfunction: A hypothesis-generating study. Respir Care 2019;64:115-6.
doi: 10.4187/respcare.06510

[11] Guizilini S, Viceconte M, Esperança GT, Bolzan DW, Vidotto M, Moreira RS, *et al*. Pleural subxyphoid drain confers better pulmonary function and clinical outcomes in chronic obstructive pulmonary disease after off-pump coronary artery bypass grafting: A randomized controlled trial. Rev Bras Cir Cardiovasc 2014;29:588-94.
doi: 10.5935/1678-9741.20140047

[12] Barbas CV, Isola AM, Farias AM, Cavalcanti AB, Gama AMCD. Diretrizes brasileiras de ventilação mecânica. Associação de medicina intensiva brasileira e sociedade brasileira de pneumologia e tisiologia. Parte 2. J Bras Pneumol São Paulo 2013;1:1-140.
doi: 10.5935/0103-507X.20140017

[13] ATS Committee on Proficiency Standards for Clinical Pulmonary Function Laboratories. ATS statement: Guidelines for the six-minute walk test. Am J Respir Crit Care Med 2002;166:111-7.
doi: 10.1164/ajrccm.166.1.at1102

[14] Riberto M, Miyazaki MH, Jucá SSH, Sakamoto H, Pinto PPN, Battistela LR. Validation of the Brazilian version of the functional independence measure. Acta Fisiatr 2004;11(2):72-6.
doi: 10.5935/0104-7795.20040003

[15] Medical Research Council. Aids to the Investigation of Peripheral Nerve Injuries. War Memorandum. 2nd ed. London: HMSO; 1943.

[16] De Araújo-Filho AA, De Cerqueira-Neto ML, Cacau LA, Oliveira GU, Cerqueira TC, De Santana-Filho VJ. Effect of prophylactic non-invasive mechanical ventilation on functional capacity after heart valve replacement: A clinical trial. Clinics 2017;72:618-23.
doi: 10.6061/clinics/2017(10)05

[17] Landoni G, Zangrillo A, Cabrini L. Noninvasive ventilation after cardiac and thoracic surgery in adult patients: A review. J Cardiothorac Vasc Anesth 2012;26:917-22.
doi: 10.1053/j.jvca.2011.06.003

[18] Reis HV, Borghi-Silva A, Catai AM, Reis MS. Impact of CPAP on physical exercise tolerance and sympathetic-vagal balance in patients with chronic heart failure. Braz J Phys Ther 2014;18:218-27.
doi: 10.1590/bjpt-rbf.2014.0037

[19] Franco AM, Torres FC, Simon IS, Morales D, Rodrigues AJ. Avaliação da ventilação não-invasiva com dois níveis de pressão positiva nas vias aéreas após cirurgia cardíaca. Rev Bras Cir Cardiovasc 2011;26(4):582-90.
doi: 10.5935/1678-9741.20110048

[20] Gremeaux V, Troisgros O, Benaïm S, Hannequin A, Laurent Y, Casillas JM, e*t al*. Determining the minimal clinically important difference for the six-minute walk test and the 200-meter fast-walk test during cardiac rehabilitation program in coronary artery disease patients after acute coronary syndrome. Arch Phys Med Rehabil 2011;92:611-9.
doi: 10.1016/j.apmr.2010.11.023

[21] Nasrala MLS, Bolzan DW, Lage YG, Prado FS, Arena R, Lima PRL, *et al*. Extended-time of noninvasive positive pressure ventilation improves tissue perfusion after coronary artery bypass surgery: A randomized clinical trial. Braz J Cardiovasc Surg 2018;33:250-7.
doi: 10.21470/1678-9741-2017-0232

[22] Shoji CY, Figuereido LCD, Calixtre EM, Rodrigues CDA, Falcão ALE, Martins PP, *et al*. Reintubation of patients undergoing cardiac surgery: A retrospective analysis. Rev Bras Ter Intensiva 2017;29:180-187.
doi: 10.5935/0103-507X.20170028

[23] Wu Q, Xiang G, Song J, Xie L, Wu X, Hao S, *et al*. Effects of non-invasive ventilation in subjects undergoing cardiac surgery on length of hospital stay and cardiac-pulmonary complications: A systematic review and meta-analysis. J Thorac Dis 2020;12:1507-19.
doi: 10.21037/jtd.2020.02.30

[24] Zarbock A, Mueller E, Netzer S, Gabriel A, Feindt P, Kindgen-Milles D. Prophylactic nasal continuous positive airway pressure following cardiac surgery protects from postoperative pulmonary complications: A prospective, randomized, controlled trial in 500 patients. Chest 2009;135:1252-9.
doi: 10.1378/chest.08-1602

[25] Cordeiro ALL, Gruska CA, Ysla P, Queiroz A, Nogueira SCO, Leite MC, *et al*. Effect of different levels of peep on oxygenation during non-invasive ventilation in patients submitted to CABG surgery: Randomized clinical trial. Braz J Cardiovasc Surg 2017;32:295-300.
doi: 10.21470/1678-9741-2016-0038

[26] Liu Q, Shan M, Liu J, Cui L, Lan C. Prophylactic noninvasive ventilation versus conventional care in patients after cardiac surgery. J Surg Res 2020;246:384-94.
doi: 10.1016/j.jss.2019.09.008

[27] Laizo A, Delgado FEF, Rocha GM. Complications that increase the length of stay in the intensive care unit in cardiac surgery. Braz J Cardiovasc Surg 2010;25:166-71.
doi: 10.1590/S0102-76382010000200007

[28] Cabrini L, Plumari VP, Nobile L, Olper L, Pasin L, Bocchino S, *et al*. Non-invasive ventilation in cardiac surgery: A concise review. Heart Lung Vessel 2013;5:137-41.

DOI: http://doi.org/10.36922/jctr.24.00011

Journal of Clinical and Translational Research 2024; 10(6): 343-347

Journal of Clinical and Translational Research

Journal homepage: http://www.jctres.com/en/home

ORIGINAL ARTICLE

Correlation between students' Bruininks–Oseretsky test scores and cavity preparation performance on layered base plate blocks

Ammar Musawi[1*], Rami Al-Saidi[2], Shalini Bhatia[3], Kneka Smith[4], Patricia Inks[5], Hamid Nurrohman[6]

[1]*Missouri School of Dentistry and Oral Health, A.T. Still University, Kirksville, Missouri, United States of America,* [2]*Private Practice, Dental Implants of Ocala, Florida, United States of America,* [3]*Department of Biostatistics, St. Jude Children's Research Hospital, Memphis, Tennessee, United States of America,* [4]*MaineHealth Maine Medical Center, Portland, Maine, United States of America,* [5]*Department of Dental Operations, Healthcare Network, Naples, Florida, United States of America,* [6]*Department of Restorative Dentistry and Prosthodontics, School of Dentistry, University of Texas, Houston, Texas, United States of America*

ARTICLE INFO

Article history:
Received: March 6, 2024
Accepted: October 29, 2024
Published Online: December 10, 2024

Keywords:
Bruininks–Oseretsky test 2
Innate hand skills
Dental admission

**Corresponding author:*
Ammar Musawi
Missouri School of Dentistry and Oral Health, A.T. Still University, Kirksville, Missouri, United States of America.
Email: amusawi@atsu.edu

ABSTRACT

Background: Hand skills are a crucial competency for practicing dentistry. However, assessing candidates' skill levels during dental school admissions in the United States is not a standard criterion due to the absence of accurate tools. Consequently, some students struggle to develop these skills, leading to dropouts, financial losses (i.e., tuition and living expenses), and an increased burden on the faculty to support struggling students.
Aim: This study aims to assess the correlation between student scores on the Bruininks–Oseretsky Test of Motor Proficiency 2 (BOT-2) and cavity preparation performance on Learn-A-Prep II (LAP II) layered base plate blocks.
Methods: First-year dental students completed the BOT-2. A total score and subtest scores, evaluating fine motor precision (seven tasks), fine motor integration (eight tasks), and manual dexterity (five tasks), were calculated. Students were also given basic handpiece training and visual and verbal project criteria for using the LAP II. They were then instructed to independently prepare LAP II patterns within the pattern lines at a specified depth. Scores for the BOT-2 were compared with LAP II performance (excellent, moderate, or poor).
Results: Forty-two students participated in the study. A general linear model (a combination of both regression and analysis of variance tests) was used to compare outcomes between students with excellent and poor performance. A strong correlation was found between the BOT-2 total scores and LAP II performance ($P = 0.04$). No correlation was found when comparing the performance of moderate students with that of excellent and poor students. The manual dexterity BOT-2 scores were correlated with LAP II performance ($P = 0.01$), but fine motor precision and fine motor integration BOT-2 scores were not (both $P > 0.12$).
Conclusion: Results of the current study suggested that scores for the BOT-2 manual dexterity subtest reliably identified dental students with either excellent or poor hand skills. Dental educators should consider using the BOT-2 as a predictive tool to identify the innate hand skills of students.
Relevance for Patients: Identifying candidates with strong hand skills during dental school admissions enables schools to select students better equipped to excel in clinical training and enhance the quality of patient care provided.

1. Introduction

Dental education involves a complex combination of didactic and practical training. Worldwide, dental school admission is often based on academic success, cognitive factors, and interpersonal characteristics. In the United States of America (USA), dental schools offer 4-year programs that traditionally rely on the predental cumulative

DOI: http://doi.org/10.36922/jctr.24.00009

and science grade point averages of applicants and their dental admission test scores [1]. However, these factors have been found to have limited predictive value for academic performance in dental school [2]. Thus, when dental schools are considering applicants for admission, the American Dental Education Association recommends the use of non-cognitive methods alongside traditional cognitive measures [3]. Dental schools assess students' hand skills through a series of regularly administered practical exams that increase in difficulty each semester of the program to ensure students' clinical readiness for patient procedures.

Several studies have attempted to identify a screening tool that can precisely predict the future performance of students in preclinical practical courses [4,5]. However, there is no consensus on the best predictive test of manual dexterity [6]. In a previous study [7], the Bruininks–Oseretsky Test of Motor Proficiency, Second Edition (BOT-2) was used as a screening tool to assess the manual dexterity of prospective and preclinical dental students. The study [7] employed this test because it is a norm-referenced, standardized tool that assesses motor performance. More specifically, it measures fine manual control, manual coordination, body coordination, strength, and agility [8-10]. However, results of the study [7] suggested BOT-2 was not completely predictive of the manual skills of prospective or preclinical dental students. Further, a stated limitation was the comparison of results between different classes of students [7]. Therefore, additional research is necessary to assess the validity of the BOT-2 tool for predicting the preclinical performance of dental students in a single cohort of participants, such as 1st-year students. More research is also necessary to identify and validate standardized, non-cognitive instruments that predict dental student performance during admissions.

In addition to identifying screening tools that assess the manual dexterity of dental students, tools are also needed to develop their hand skills. A variety of lead-up activities have been developed to assist in the early development of psychomotor skills for operative dentistry [11]. For instance, the Learn-A-Prep II (LAP II) was developed as a training aid for use during the initial instructional levels of dental education. This tool uses layered base plate blocks of different colors and material hardness to mimic enamel, dentin, and pulp tissue. The overall goal of the design of these blocks is to foster student understanding of movement through vertical and horizontal spaces as they develop the ability to create precise 3D preparations. To the best of our knowledge, few studies have investigated the potential benefit of using the LAP II as a predictive tool of student performance during the dental admission process [12,13]. Further, based on our experience, a high percentage of students drop out of dental school due to failure to achieve competency in the practical exams required for progression through the program. Therefore, having tools that could identify students with poor hand skills before they are admitted to dental school would be beneficial. Such knowledge could save students' time and money, while reducing monetary losses dental schools face due to dropouts. Ultimately, better predictive tools would improve the quality of oral care services provided by dental school students and graduates [14].

Since tools that predict dental students' hand skills and performance have the potential to advance both dental education and clinical practice, studies are necessary to identify these tools. Therefore, the purpose of the current study was to assess the correlation between student BOT-2 scores and cavity preparation performance on LAP II layered base plate blocks. We hypothesized that the correlation between BOT-2 and LAP II scores would serve as a non-cognitive indicator of innate hand skills, helping dental schools make more efficient student admission decisions. There is no information on any dental school utilizing the BOT-2 test for dental school students or its validity in the discussed context.

2. Methods

The current study was reviewed by the local institutional review board and considered exempt. Only 1st-year dental students from a single class were eligible for participation, and all participants signed an approved informed consent form before the study. Demographic information about the gender and age of students was collected. Participation was voluntary/mandatory, and student performance in the study did not affect course grades.

All students in the class were included in the study; inclusion criteria were simply being part of the cohort of the dental students that was enrolled that year. There were no exclusion criteria set for this study. Students can only be excluded if they choose not to participate and do not consent to their scores being used in the study.

To assess the manual dexterity of dental students, we used BOT-2 as it is the most precise and comprehensive measure of motor skills (both gross and fine). BOT-2 is an easy-to-administer test and contains subtests and challenging game-like tasks. We included three of the BOT-2 subtests in the current study: fine motor precision (seven tasks), fine motor integration (eight tasks), and manual dexterity (five tasks); each administered to 1st-year dental students (D1 class 2017 and D1 class 2018 [n = 42]). Scores for tasks within each subtest were added to obtain a total score for each subtest, and those scores were also compared. An experienced faculty member, calibrated in administering and scoring BOT-2, conducted the tests.

To evaluate the hand skills of dental students, LAP II layered base plate blocks (Whip Mix Corporation, USA) were used as a cavity preparation project (Figure 1). For this test, students used the LAP II to prepare a cavity representing class I on the lower molar tooth on the LAP II block. The preparation criteria included following the outline provided, with 2-mm depth, straight smooth walls, and a flat smooth floor. Students were instructed to prepare the various shapes up to, but not into or beyond, the pattern outline, while maintaining a constant depth throughout the artificial enamel without penetrating the dentin. The outlined shape used for this test was chosen because it resembled an operative dentistry class I preparation. Before the task, students were introduced to LAP II and received the same instructions from a single faculty member about using a dental handpiece. Specifically, students were taught how to hold a handpiece and use the simulation unit. Next, verbal instructions and a live demonstration were provided to teach students the

DOI: http://doi.org/10.36922/jctr.24.00009

steps for LAP II pattern preparation. They were taught how to prepare a flat pulpal floor, produce a proper outline form, achieve a proper cavity wall angulation outline for the preparation, reach the ideal pulpal depth and smoothness, and use a perio probe to measure the height of the walls.

Students then practiced preparing a specific LAP II pattern under direct faculty supervision. This practice exercise was designed for students to familiarize themselves with the handpiece and LAP II preparation. The supervising faculty did not provide feedback on the preparation quality but did provide feedback about the proper use of the simulation unit, handpiece, and bur. During the activity, dental handpieces were preset to the same settings and speed (20000 rpm) for all students, and all students used the same bur (330 Carbide). A faculty member, who was experienced with the standardized parameters of the LAP II, administered and scored the activity.

The BOT-2 and LAP II tests were administered to 1st-year students during orientation. Both tests were introduced to students as "a fun activity." Student results for BOT2 were calculated as a total score and as separate total scores for each subtest. Student scores for LAP II performance were categorized as excellent (when the preparation was perfect or had one minor deviation from ideal), moderate (when the preparation had only one moderate error or multiple minor deviations from ideal), or poor (when the preparation had a major error or multiple moderate errors, resembling a clinically unacceptable performance). A single, blinded faculty member graded the work of all students using a simplified rubric.

Overall BOT-2 scores were calculated using the median and interquartile range (IQR). The Wilcoxon rank sum test was used to compare the BOT-2 total score and the total score for each subtest. Analysis of variance was used to compare total BOT-2 scores for each subtest with student performance category scores on the LAP II. The Tukey test was used for *post-hoc* comparisons, and data were reported as the mean difference with the associated 95% confidence interval (CI). A generalized linear model was used to investigate the correlation between student performance on the LAP II preparation activity and their total BOT-2 score or total BOT-2 subtest scores. Analyses were performed using SAS version 9.4 (SAS Inc., USA). A $P < 0.05$ was considered statistically significant.

Figure 1. Learn-A-Prep II layered base plate block

3. Results

A total of 42 dental students (22 males and 20 females) from the D1 class of 2017 participated in this study; one female student was excluded due to her inability to perform some of the BOT-2 tasks required for the study. The mean age of the students was 24 years old. Using the general linear model, which is a mixture of both regression and analysis of variance, a correlation was found between the total BOT-2 scores and LAP II cavity preparation performance (Figure 2).

Student scores on the BOT-2 are presented in Table 1. For the fine motor precision subtest, only drawing lines through a path (curved; median [IQR]: 7 [1]) and connecting dots (median [IQR]: 7 [0]) were significant (both $P < 0.001$). For the fine motor integration subtest, only copying overlapping circles (median [IQR]: 5 [1]; $P = 0.03$) was significant. For the manual dexterity subtest, only the total score was significantly different (median [IQR]: 34 [3]; $P = 0.007$).

For LAP II, 17 students had excellent scores, 16 had moderate scores, and nine had poor scores. Comparisons between the BOT-2 subtest scores and the LAP II scoring categories are presented in Table 2. A mean difference in total scores was found only for the BOT-2 manual dexterity subtest ($P = 0.01$). Using the Tukey test adjustment, a difference was found between students with excellent and poor scores (mean difference [95% CI]: 3.5 [0.7 – 6.2]; $P = 0.01$).

4. Discussion

The current study assessed the correlation between student BOT-2 scores and cavity preparation performance on LAP II layered base plate blocks to determine whether these tests could be used as a non-cognitive indicator of preclinical operative dentistry performance during the dental school admissions process. The mean age of the students was 24 years old, which

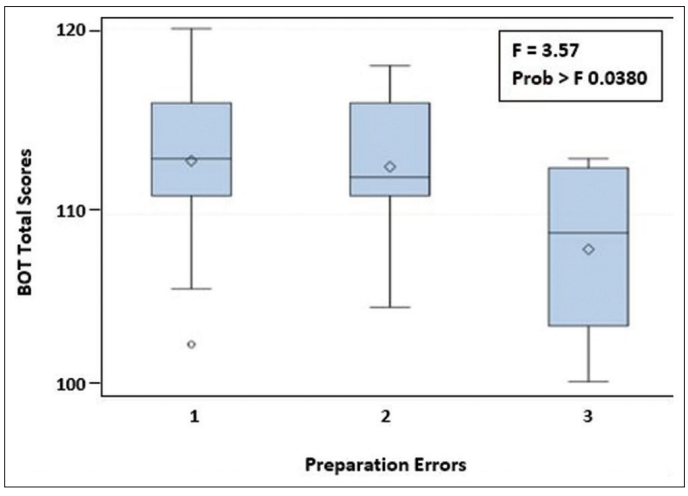

Figure 2. General linear model results for the correlation between the Bruininks–Oseretsky test of motor proficiency 2 and learn-A-prep II

DOI: http://doi.org/10.36922/jctr.24.00009

is higher than that of students in other nations, due to the differences in the admission criteria and processes followed in the USA. Results suggested that the manual dexterity subtest of BOT-2 was able to differentiate between students with excellent (innate hand skills) and poor (no innate hand skills) LAP II scores. No statistically significant differences between scores for the BOT-2 and LAP II were found for the other two BOT-2 subtests, i.e., fine motor precision and fine motor integration.

Table 1. Comparison of Bruininks–Oseretsky test of motor proficiency 2 (BOT-2) scores from two different classes

BOT-2 subtest	Median (IQR)		*P*-value
	D11	D12	
Fine motor precision	40 (2)	40 (2)	0.4
Filling in shape (circle)	3 (0)	3 (1)	0.7
Filling in shape (star)	3 (0)	3 (0)	0.3
Drawing lines through a path (crooked)	7 (0)	7 (0)	0.3
Drawing lines through a path (curved)	7 (1)	7 (0)	0.0007
Connecting dots	7 (0)	6 (1)	< 0.0001
Folding paper	7 (0)	7 (0)	0.2
Cutting out a circle	7 (0)	7 (0)	0.4
Fine motor integration	37 (3)	38 (3)	0.4
Copying a circle	4 (1)	4 (0)	0.7
Copying a square	5 (0)	5 (0)	0.09
Copying overlapping circle	5 (1)	6 (1)	0.03
Copying a wavy line	4 (0)	4 (0)	0.1
Copying a triangle	5 (0)	5 (0)	0.2
Copying a diamond	5 (0)	5 (0)	1.0
Copying a star	4 (1)	4 (1)	0.3
Copying overlapping pencils	5 (0)	5 (1)	0.3
Manual dexterity	34 (3)	35 (4)	0.007
Making dots in a circle	9 (1)	9 (1)	0.3
Transferring pennies	7 (1)	8 (2)	0.08
Placing pegs into a pegboard	6 (2)	6 (1)	0.08
Sorting cards	7 (0)	7 (1)	0.1
Stringing blocks	5 (0)	5 (1)	0.07
Overall	110 (8)	112 (6)	0.09

Note: D11 denotes the D1 class of 2017; D12 denotes the D1 class of 2018.
Abbreviation: IQR: Interquartile range.

Our findings support a previous study by Boushell *et al*., [12] which reported the potential benefits of using LAP II as a predictive training tool of psychomotor performance in an operative dentistry course. However, in that study, [12] students were instructed to independently prepare LAP II patterns within the pattern lines and at a specified depth only. In the current study, we had students prepare a flat pulpal floor, produce a proper outline form, achieve a proper cavity wall angulation (convergence), and reach the ideal pulpal depth (2 mm) and smoothness, allowing us to compare the various components of cavity preparation to better clarify the predictive value of LAP II.

The findings of the current study contradict the results of a similar study by Musawi *et al*. [7] In that study, [7] BOT-2 was not a reliable predictor of the hand skills of new dental students. However, the study [7] compared the BOT-2 scores of 1st-year and 2nd-year students to determine a correlation. The study found no differences, which may be due to the different hand skill levels between the two groups of students. [7] Therefore, the current study only compared the scores of 1st-year students.

The current study had several limitations. The main limitation was our small sample size of 42 students. Since data from one student were excluded, data from only 41 students were included in our analyses. A larger sample size or repeating the study with more classes would be useful to verify current findings. The wide age range of the participants might also be an influential factor in the results of the study. Although our findings for student performance during the LAP II activity were similar to those of Boushell *et al*. and Khalaf *et al*., [12,13] the results may not accurately represent the actual hand skills of students. Instead, our results may be a better representation of their hand skill level and comprehension of the provided instructions for preparing the cavity. To better determine the source of LAP II results, future studies should investigate student comprehension of instructions. Data from such studies would be particularly useful for dental

Table 2. Correlation between Bruininks-Oseretsky test of motor proficiency 2 (BOT-2) scores and students' performance on the Learn-A-Prep II (LAP II) block

BOT-2 subtest	LAP II performance comparison	Mean difference	*P*-value	95% CI	
				Lower bound	Upper bound
Fine motor precision	Overall *F*-test	-	0.1	-	-
	Excellent versus moderate	0.01	1.0	−1.2	1.3
	Excellent versus (major) poor	1.2	0.2	−0.3	2.7
	Moderate versus poor	1.2	0.2	−0.4	2.7
Fine motor integration	Overall *F*-test	-	0.4	-	-
	Excellent versus moderate	−1.0	0.5	−3.0	1.0
	Excellent versus poor	0.1	1.0	−2.4	2.5
	Moderate versus poor	1.1	0.6	−1.4	3.6
Manual dexterity	Overall *F*-test	-	0.01	-	-
	Excellent versus moderate	1.3	0.3	−0.9	3.5
	Excellent versus poor	3.5	0.01	0.7	6.2
	Moderate versus poor	2.2	0.1	−0.6	5.0

Abbreviation: CI: Confidence interval.

DOI: http://doi.org/10.36922/jctr.24.00009

educators, as comprehension is considered a crucial factor for excellent performance as a dental student and future professional.

5. Conclusion

Results of the current study suggested that the manual dexterity subtest of BOT-2 may be able to reliably predict the level of innate hand skill and task comprehension abilities of prospective dental students during the admissions process. Therefore, dental educators should consider using BOT-2 as a predictive tool to identify the innate hand skills of students. However, additional studies with larger sample sizes are necessary to verify the findings of the current study. Further, dental schools should consider using this combination of BOT-2 and LAP II as part of the admissions process to improve student retention and, ultimately, the quality of oral care provided to patients.

Acknowledgments

The authors would like to acknowledge the ATSU Research and Sponsored Programs for their support of the present study.

Funding

None.

Conflicts of Interest

The authors reported no competing interests.

Ethics Approval and Consent to Participate

This study was exempted by the ATSU IRB (A.T. Still University) under section 45CFR46.101(b)(2). No further review was necessary. Consent was provided by the students participating in the study and their signatures were acquired.

Consent for Publication

Consent was acquired from the study participants to publish their data.

Availability of Data

Data is available from the corresponding author upon reasonable request.

References

[1] Ranney RR, Wilson MB, Bennett RB. Evaluation of Applicants to Predoctoral Dental Education Programs: Review of the Literature. J Dent Educ 2005;69:1095-106.
doi: 10.1002/j.0022-0337.2005.69.10.tb04010.x

[2] Curtis DA, Lind SL, Plesh O, Finzen FC. Correlation of Admissions Criteria with Academic Performance in Dental Students. J Dent Educ 2007;71:1314-21.
doi: 10.1002/j.0022-0337.2007.71.10.tb04395.x

[3] ADEA Policy Statements: Recommendations and Guidelines for Academic Dental institutions. J Dent Educ 2017;81:869-81.
doi: 10.1002/j.0022-0337.2017.81.7.tb06305.x

[4] Lundergan WP, Soderstrom EJ, Chambers DW. Tweezer Dexterity Aptitude of Dental Students. J Dent Educ 2007;71:1090-7.
doi: 10.1002/j.0022-0337.2007.71.8.tb04375.x

[5] Kothe C, Hissbach J, Hampe W. Prediction of Practical Performance in Preclinical Laboratory Courses: The Return of Wire Bending for Admission of Dental Students in Hamburg. GMS Z Med Ausbild 2014;31:Doc22.
doi: 10.3205/zma000914

[6] Suksudaj N, Townsend GC, Kaidonis J, Lekkas D, Winning TA. Acquiring Psychomotor Skills in Operative Dentistry: Do Innate Ability and Motivation Matter? Eur J Dent Educ 2012;16:e18794.
doi: 10.1111/j.1600-0579.2011.00696.x

[7] Musawi A, Barrett T, Nurrohman H, Bhatia S, Smith K. Assessing Likelihood of Using the Bruininks-Oseretsky Test of Motor Proficiency to Predict Preclinical Performance of Dental Students. Clin Exp Dent Res 2019;5:513-8.
doi: 10.1002/cre2.217

[8] Bruininks RH. Bruininks-Oseretsky Test of Motor Proficiency: Examiner's Manual. OCLC Number: 4491119. Circle Pines, MN: American Guidance Service; 1978.

[9] Bruininks R, Bruininks B. Bruininks-Oseretsky Test of Motor Proficiency. 2nd ed. Minneapolis, MN: NCS Pearson; 2005.
doi: 10.1300/J006v27n04_06

[10] Deitz JC, Kartin D, Kopp K. Review of the bruininks-oseretsky test of motor proficiency, second edition (BOT-2). Phys Occup Ther Pediatr 2007;27:87-102.
doi: 10.1080/J006v27n04_06

[11] Feil P, Reed T, Hart JK. The transfer effect of leadup activities. J Dent Educ 1990;54(10):609-11.
doi: 10.1002/j.0022-0337.1990.54.10.tb02470.x

[12] Boushell LW, Walter R, Phillips C. Learn-a-prep II as a predictor of psychomotor performance in a restorative dentistry course. J Dent Educ 2011;75:1362-9.
doi: 10.1002/j.0022-0337.2011.75.10.tb05182.x

[13] Khalaf ME, Alkhubaizi Q, Alomari QD. Layered Base Plate Blocks and Operative Dentistry Skills. J Contemp Dent Pract 2018;19:554-9.
doi: 10.5005/jp-journals-10024-2298

[14] Portelli M, Matarese G, Militi A, Cordasco G, Lucchese A. A Proportional Correlation Index for Space Analysis in Mixed Dentition Derived from an Italian Population Sample. Eur J Paediatr Dent 2012;13:113-7.

Journal of Clinical and Translational Research 2024; 10(6): 348-356

Journal of Clinical and Translational Research

Journal homepage: http://www.jctres.com/en/home

ORIGINAL ARTICLE

Effect of high-intensity interval and endurance training with MitoQ on mitochondrial dynamics in rat muscle

Soheil Aminizadeh[1], Hamid Najafipour[2], Yaser Masoumi-Ardakani[3], Beydolah Shahouzehi[4]*, Mohammad Pourranjbar[5]

[1]Physiology Research Center, Institute of Neuropharmacology, Department of Physiology and Pharmacology, Afzalipour School of Medicine, Kerman University of Medical Sciences, Kerman, Iran, [2]Cardiovascular Research Center, Institute of Basic and Clinical Physiology Sciences, Kerman University of Medical Sciences, Kerman, Iran, [3]Endocrinology and Metabolism Research Center, Institute of Basic and Clinical Physiology Sciences, Kerman University of Medical Sciences, Kerman, Iran, [4]Gastroenterology and Hepatology Research Center, Institute of Basic and Clinical Physiology Sciences, Kerman University of Medical Sciences, Kerman, Iran, [5]Department of Physical Education, Faculty of Medicine and Physiology Research Center, Kerman University of Medical Sciences, Kerman, Iran

ARTICLE INFO

Article history:
Submitted: July 22, 2024
Accepted: December 9, 2024
Published Online: December 24, 2024

Keywords:
MitoQ
Exercise training
Fission
Fusion
Mitochondrial dynamic

**Corresponding author:*
Beydolah Shahouzehi
Gastroenterology and Hepatology Research Center, Institute of Basic and Clinical Physiology Sciences, Kerman University of Medical Sciences, Kerman, Iran.
Email: bshahouzehi@gmail.com

ABSTRACT

Background and Aim: Mitochondria play an important role in signaling and metabolic pathways in skeletal muscle. In this study, the effects of MitoQ supplementation alone and in combination with endurance training (ET) or high-intensity interval training (HIIT) were investigated in relation to the process of mitochondrial quality control in the gastrocnemius muscle of male rats.

Methods: Animals were assigned into 6 groups (n = 7): Control, MitoQ, ET, ET + MitoQ, HIIT, and HIIT + MitoQ. The gene and protein expression were quantified using real-time polymerase chain reaction ($2^{-\Delta\Delta CT}$) and Western blot analysis, respectively. Statistical analysis was performed using one-way analysis of variance.

Results: ET significantly increased protein expression of dynamin-related protein 1 (DRP1) and mitofusin1 (MFN1) and gene expression of optic atrophy Type 1 (*Opa1*) in skeletal muscle, when compared to the control group ($p < 0.001$). HIIT only increased MFN1 protein expression compared to the control group ($p < 0.0001$). MitoQ in combination with HIIT significantly increased protein expression of DRP1 and MFN1 compared to MitoQ alone ($p < 0.01$).

Conclusion: In sum, exercise training can affect mitochondrial dynamics by changing the factors involved in the fission and fusion process, and ET can improve training capacity in skeletal muscle by modulating expression of OPA1 and MFN1. While MitoQ supplementation alone did not significantly alter the mitochondrial fission-fusion process, its combination with HIIT appeared to elevate the expression of DRP1, suggesting a potential synergistic effect that warrants further investigation. Future studies should delve into the mechanisms by which MitoQ and exercise-induced stress affect mitochondrial quality control, particularly in the context of redox modulation and signaling pathways that govern mitochondrial plasticity.

Relevance for Patients: Combining MitoQ with exercise training may enhance mitochondrial function, potentially improving muscle health in patients.

1. Introduction

Regarded as dynamic organelles, mitochondria change their shape and structure in response to various metabolic stimuli. Mitochondrial structure is mainly regulated by fusion and fission cycles. These processes are tightly regulated to ensure a balance. Dysregulated fusion and fission of mitochondria is an important mechanism in the development of some diseases [1]. Mitochondrial dysfunction results in chronic

DOI: http://doi.org/10.36922/jctr.24.00044

inflammation, which leads to a vicious cycle between chronic inflammation and mitochondrial reactive oxygen species (ROS) production [2].

Exercise training provides a powerful boost to initiate the signaling pathways described above, which eventually create strong phenotypic changes in the mitochondria and improve the quantity and quality of the organelle network, leading to greater muscle health [3]. Exercise triggers an adaptive response through redox signaling that increases mitochondrial function (a combination of quality and quantity), boosting metabolism and antioxidant stores, not only allowing the organism to better control inflammation but also making it more resistant to most stressors [4]. In addition, mitochondria can be involved in the progression of sarcopenia as they are critical controllers of an assortment of variables that contribute to the etiology of the condition, such as ATP provision, oxidative stress, and apoptosis, as well as inflammation and calcium ions (Ca^{2+}) handling [5]. Regular aerobic exercise can relieve inveterate irritation in skeletal muscle by activating mitochondrial quality control processes to improve organelle phenotypes, with the possibility of reducing the release of mitochondrial damage-associated molecular patterns (mtDAMPs). This could attenuate inflammasome activation and counteract the detrimental effects of chronic inflammation on muscle development and function [6].

Mitochondrial stress, a consequence of stimuli such as exercise training, leads to the release of significant stress signals including ROS and Ca^{2+}, which are crucial in regulating cellular signaling cascades [7]. However, excessive mitochondrial stress or failure of the adaptive response may result in irreversible mitochondrial damage and the release of apoptotic signals, ultimately triggering cellular apoptosis [7]. During the apoptosis process, mitochondria are influenced by dynamic changes in various proteins, such as dynamin-related protein 1 (Drp1) and the apoptotic regulators BAX and BCL-2 [8]. In addition, peroxisome proliferator-activated receptor gamma coactivator 1-alpha (PGC-1α) is essential for regulating key factors that orchestrate mitochondrial dynamics and mitophagy, such as mitofusin 2 (MFN2), DRP1, PTEN-induced putative kinase protein 1 (PINK1), and parkin [9]. Furthermore, an interplay between PGC-1α and nuclear factor erythroid 2-related factor 2 (NRF2) is crucial for modulating mitochondrial stress adaptations, highlighting their roles in promoting cell survival and reducing oxidative stress [10]. Inhibiting mitochondrial fission can delay downstream caspase activation and subsequent apoptosis, while overexpression of mitofusin 1 (MFN1) or MFN2 may postpone apoptotic cell death. The fusion process permits the integration of fragmented, viable mitochondria back into the mitochondrial network [11]. Mitochondrial fusion is regulated by two members of the large GTPase family, MFN1 and MFN2 [12]. The genetic deletion of mitofusins leads to the accumulation of dysfunctional mitochondria and subsequent cell damage [13]. MFN2 expression can be downregulated by growth factors, cytokines, and lipid availability, but upregulated by exercise and energy consumption [14]. In addition, several intracellular pathways, including those associated with cell cycle progression, mitochondrial bioenergetics maintenance, apoptosis, and autophagy, affect MFN2 expression [15]. Moreover, mitochondrial fission is influenced by proteins such as mitochondrial fission 1 protein (FIS1) and DRP1, while the fusion process is mediated by the optic atrophy 1 (OPA1) and mitofusins protein family [16].

MitoQ, a mitochondria-targeted antioxidant supplement, scavenges free radicals, reduces oxidant production and lipid peroxidation, and removes peroxide nitrite [17], being ~800-fold more effective than untargeted antioxidants. It condenses on the matrix surface of the inner mitochondrial membrane and exerts antioxidative effects by oxidizing ubiquinol to ubiquinone [18]. It has been shown that chronic administration of MitoQ ameliorates mitochondrial ROS production in the skeletal muscles of middle-aged men [19]. The MitoQ supplement is an advanced orally used antioxidant that protects the mitochondria as the energy production site. MitoQ is designed to accumulate in the mitochondrial matrix and ultimately exert beneficial effects by electron reduction and free radical attenuation [20]. MitoQ reduces the production of ROS and imbalance in mitochondrial membrane potential [21], prevents endothelial cell death, and normalizes vascular function in various diseases [22]. However, the effectiveness of MitoQ supplementation is not fully understood. In another study, the effect of MitoQ in combination with endurance training (ET) on male athletes showed that MitoQ supplementation increases the antioxidant capacity of skeletal muscle [23].

Scientists have utilized a variety of exercise training protocols to challenge skeletal muscle to determine the effect on acute mitochondrial signaling and chronic mitochondrial adaptation. Moore *et al.* [24] showed that regulators of mitochondrial fission, *Fis1*, and *Dnm1L* (encodes the protein DRP1) were upregulated in the skeletal muscle of mice after ET for 90 min, although only *Fis1* expression remained elevated during the 3-h recovery period, and *Dnm1L* expression returned to baseline (90-min exercise training + 3-h rest). In contrast to *Fis1*, mitochondrial fission factor (*Mff*) expression was reduced during acute exercise and this reduction in expression reached statistical significance during the 3-h recovery period (90-min exercise training + 3-h rest) [24]. Endurance exercise (one session) can be sufficient to induce changes in the mitochondrial life cycle including mitochondrial fission signaling through Drp1. Furthermore, lacking Drp1 reduced exercise performance and altered training-induced adaptations [24]. In mouse models of fission-fusion incompetence, researchers have shown that impaired dynamic flux of mitochondrial remodeling is associated with derangements in metabolism and insulin sensitivity. Because the processes of mitochondrial fission, fusion, biogenesis, and quality control are interdependent, strategies aimed at enhancing mitochondrial lifecycle flux capacity may be effective in combating diseases associated with metabolic dysfunction.

Mitochondrial health and function are critical for overall cellular performance, and exercise training is a well-known stimulus that can enhance mitochondrial quality. The effects of different training modalities, specifically ET and HIIT, on mitochondrial dynamics remain largely unexplored. In this

DOI: http://doi.org/10.36922/jctr.24.00044

study, we hypothesize that MitoQ supplementation, both as an isolated treatment and combined treatment with ET and HIIT, will significantly influence mitochondrial dynamics within the gastrocnemius muscle of male rats. Moreover, we propose that the distinct characteristics of each training modality may differentially impact mitochondrial dynamic when paired with MitoQ supplementation. This study aims to provide deeper insights into how these interventions can enhance mitochondrial function.

2. Materials and Methods

2.1. Animals

Forty-two male Wistar rats, each weighing 200 ± 10 g and aged 8 weeks, were obtained from the Physiology Research Center (Karman, Iran) and maintained under standard conditions as follows: 12-h light/dark cycle; 23 ± 2°C; and humidity of 55 ± 10%. Animals were randomly divided into 6 groups ($n = 7$): (i) Untreated control (CTL); (ii) MitoQ, which received 250 μM MitoQ in drinking water for 8 weeks; (iii) ET, which performed ET; (iv) ET + MitoQ; (v) HIIT, which performed high-intensity interval training; and (vi) HIIT + MitoQ. In the ET groups, the rats were trained on a treadmill for 8 weeks, 5 days/week, 50 min/day. Animals in the HIIT groups performed training (80 – 90% of V_{max} in 2-min intervals) 5 days/week for 8 weeks by running on a treadmill. The animal procedure was approved by the Animal Care Committee of the Ethics Committee of Kerman University of Medical Sciences (IR.KMU.REC.1400.292). All methods were performed in adherence to the ARRIVE (Animal Research: Reporting of In Vivo Experiments) guidelines 2.0.

2.2. MitoQ treatment

MitoQ (MitoQ Ltd, New Zealand) was given to animals at a dose of 250 μM in drinking water [25]. To assess the targeting of MitoQ in tissues, the concentration of MitoQ was measured in the whole lysate tissues by means of high-performance liquid chromatography-mass spectrometry (HPLC-MS) [26]. For HPLC-MS calibration, we used the MitoQ internal standard (MRC Mitochondrial Biology Unit and Department of Medicine, University of Cambridge), and the tissue levels of MitoQ in the CTL group and MitoQ group were 0 and 5.68 ± 0.81 pmol/100 mg protein, respectively.

2.3. Training protocol

The rats' familiarization to adapt to the training on treadmill lasted 2 weeks, with each session set at a speed of 15 m/min for 15 min. The intensity of exercise training was calculated by measuring V_{max}. For calculation of the intensity, the speed test started with a warm-up of 10 m/min and then increased (3 m/min) till exhaustion [27]. Blood lactate levels were measured by a lactometer (Lactate Scout Company/Code: 37, Germany) directly after incremental test, and levels above 6 mmol/L were considered high intensity [28]. For HIIT, each session consisted of ten 2-min work bouts/day at 80 – 90% of V_{max} and separated by 2-min rest periods, 5 days/week for 8 weeks [29]. In the ET groups, rats were trained on a treadmill for 8 weeks, 5 days/week, 50 min/day (speed at the last week: 65 – 70% of V_{max}). The iso-distance method was used for two protocols to unify two types of the training protocol. Forty-eight hours after the end of the final training session, animals were anesthetized and sacrificed. The gastrocnemius muscle was extracted and washed with cold normal saline, frozen by liquid nitrogen, and stored at −80°C for real-time polymerase chain reaction (PCR) and Western blotting.

2.4. Western blotting

The protein levels of DRP1 and MFN1 were measured by means of Western blotting. Initially, 20 mg of skeletal muscle tissue was homogenized in cold RIPA (radioimmunoprecipitation assay) buffer containing 0.5% sodium deoxycholate, 150 mM sodium chloride (NaCl), 1.0 mM EDTA, 0.1%, 50 mM Tris-HCl, sodium dodecyl sulfate (SDS), and protease inhibitor with a pH of 7.4. After homogenization, the mixture was centrifuged (15000 rpm, 20 min, 4°C) and the supernatant was collected. Protein levels in the supernatant were determined using the Bradford method. Equal volumes of sample buffer (composed of 62.5 mM Tris-HCl, pH 6.8, 10% glycerol, 2% SDS, 0.005% bromophenol blue, and 5% β-mercaptoethanol) were mixed with the protein sample from the supernatant. The mixture was incubated at 95°C for 5 min to denature the proteins, after which each sample was loaded into the appropriate well of a 10% SDS-PAGE gel (running buffer: 25 mM Tris, 192 mM glycine, 0.1% SDS, pH 8.3). Following electrophoresis, proteins were transferred onto a polyvinylidene fluoride (PVDF) membrane using a transfer buffer (20% methanol, 25 mM Tris, 192 mM glycine, pH 8.3) under the following conditions: 200 mA for 60 min at 4°C. The blocking step was performed with a blocking solution consisting of nonfat dried milk (5% w/v) diluted in Tris-buffered saline with Tween 20 (TBST; 20 mM Tris, 150 mM NaCl, 0.1% Tween 20, pH 7.6). After blocking, the membrane was washed five times for 5 min each with TBST. For antibody detection, the PVDF membrane was incubated with primary antibodies: anti-DRP1 (sc-271583, Santa Cruz Biotechnology) and anti-MFN1 (sc-166644, Santa Cruz Biotechnology). Following five washes (5 min each) with TBST, the blots were incubated with a peroxidase-conjugated secondary antibody. After additional washing, the blots were visualized using a chemiluminescent detection system. The amount of protein was measured by quantitative density analysis and compared to β-actin (detected with anti-β-actin; sc-47778, Santa Cruz Biotechnology) as a control by Image J software [30].

2.5. Total RNA extraction and quantitative realtime PCR

The real-time PCR method was used to determine the relative expression of the genes. Total RNA was extracted from the skeletal muscle tissues using EZ-10 Spin Column Total RNA Mini-preps Kit (Bio Basic, Canada, Cat number, BS1361-SK8655). The process of RNA extraction typically involves the destruction of tissue in a chemical environment that simultaneously inactivates ribonucleases and the subsequent capture of RNA molecules using columns while leaving other

DOI: http://doi.org/10.36922/jctr.24.00044

molecules to pass through the filter. In the final step, the RNAs in the column were eluted from the column using an elution buffer and collected in sterile tubes. Then, the concentration and purity of the total extracted RNA were determined using a nanodrop instrument (Nanodrop-KLAB, South Korea). The cDNA was synthesized from total RNAs while to inhibit the RNase enzyme, RNasin (RNase inhibitor) was added to the reaction mixture (Parstous Biotechnology, Iran). Real-time PCR was performed on cDNA with polymerase enzyme, Master Mix Green (Ampliqon, Denmark), and specific primers (Table 1) for the target genes. The 18s rRNA gene was used as the housekeeping gene. After real-time PCR, Ct values were obtained for both target and reference genes. The ΔCt value indicates the difference of Ct values between the target gene and the housekeeping gene. The $2^{-\Delta\Delta CT}$ formula was used to determine relative gene expression [31].

2.6. Statistical analysis

Data are presented as mean ± standard deviation (SD). After assessing data normality with the Kolmogorov–Smirnov test, one-way analysis of variance (ANOVA) was used for comparisons between groups, followed by Tukey's post-hoc test. $p < 0.05$ was considered significant. In addition, seven rats were allocated to each group to achieve the effect size (f) of 9.044 and a study power of 95% (1-β error probe).

3. Results

Compared to the control group, the ET groups exhibited significantly increased protein levels of DRP1 ($F = 39.09$, $p < 0.0001$) and MFN1 ($F = 18.64$, $p = 0.0003$), as well as *Opa1* gene expression ($F = 4.96$, $p = 0.02$) in skeletal muscle (Figures 1A and B, and Figure 2). Meanwhile, HIIT only increased MFN1 protein levels ($F = 18.64$, $p < 0.0001$) (Figure 1B). MitoQ did not have a significant effect on the gene and protein expression (Figures 1-4). However, its combination with both exercise modalities caused significant effects. In the MitoQ-treated groups separately receiving ET or HIIT, DRP1 protein levels increased, when compared to the levels in the MitoQ group ($F = 39.09$, $p = 0.0006$; $F = 39.09$, $p < 0.0001$; respectively) (Figure 1A). Furthermore, we found that only the HIIT + MitoQ group exhibited increased MFN1 protein levels compared to the MitoQ group ($F = 18.64$, $p < 0.0001$) (Figure 1B). The gene expression of *Opa1*, *Fis1*, and *Mfn2* was unaffected by either the HIIT + MitoQ or ET + MitoQ regimens (Figures 2-4).

Table 1. Primers' sequence used in this study

Genes	Sequences (5' – 3')
Fis1	Forward: CAAGGAACTGGAGCGGCTCATT
	Reverse: GACACAGCAAGTCCGATGAGT
Opa1	Forward: CAGCTGGCAGAAGATCTCAAG
	Reverse: CATGAGCAGGATTTTGACACC
Drp1	Forward: CCAGGAATGACCAAGGTCCC
	Reverse: CCTCGTCCATCAGGTCCAAC
Mfn1	Forward: TGGGGAGGTGCTGTCTCGGA
	Reverse: ACCAATCCCGCTGGGGAGGA
Mfn2	Forward: AGCCTGGTGAGTGTGATGTG
	Reverse: CTCCGTGGTGACATCGATCC
B-actin	Forward: CCAGAGGCGTACAGGGATAG
	Reverse: CCAACCGCGAGAAGATGA

4. Discussion

The results of this study demonstrated that MitoQ alone did not change the expression of factors involved in mitochondrial dynamics, but combination of MitoQ with exercise training led to the modulation of their expression. Compared to HIIT, ET caused more remarkable changes in gene and protein expression in skeletal muscle. ET significantly increased protein expression of DRP1 and MFN1 as well as *Opa1* gene expression, while HIIT only elevated the MFN1 protein level. These findings suggest that in skeletal muscle, ET affects proteins involved in both mitochondrial fusion and fission but HIIT affects only factors involved in mitochondrial fusion.

The increase in MFN2 levels improves muscle performance following appropriate intervention. Intermittent aerobic exercise training improves energy access and reduces oxidative stress damage by increasing the expression of MFN2 and OPA1 [32]. It seems that when the rats performed ET, due to aerobic conditions (in this case, most energy production is produced by mitochondria through aerobic oxidation), the proteins related to both fusion and fission processes increased in levels and helped to improve the dynamics of mitochondria to ensure optimal mitochondrial capacity, whereas through HIIT, due to the presence of alternating aerobic and anaerobic conditions, metabolic and energy requirements were adjusted accordingly. Mitochondrial dynamics is dependent on metabolic conditions [33]. Due to this, mitochondria undergo biogenesis and fusion through PGC-1α [34,35] to meet energy requirements, and at the same time, the progression towards fission happens to remove damaged mitochondria [36]. While our results indicated that MitoQ alone did not significantly alter the expression of factors involved in mitochondrial dynamics, it is important to highlight that the interplay between exercise training and MitoQ treatment reveals critical insights into this relationship. Specifically, our findings demonstrated that the combination of exercise training and MitoQ led to enhanced expression of certain proteins involved in mitochondrial dynamics, particularly in the context of ET, which significantly increased DRP1 and MFN1 protein levels and *Opa1* gene expression [31]. This suggests that while MitoQ may not independently modify mitochondrial dynamics, it has the potential to influence these processes when combined with an exercise regimen. Furthermore, our results indicated that ET promotes both mitochondrial fusion and fission, aligning with metabolic needs, while the effects of HIIT were more central to mitochondrial fusion, reflecting a subtle understanding of how varying exercise protocols impact mitochondrial dynamics [32].

It has been reported that in skeletal muscle tissues, a session of aerobic training, despite improving mitochondrial function, does not affect mitochondrial dynamics [37]. This is in contrast with the findings of our study, and it may be due to the longer duration of the training period in our study compared to acute

DOI: http://doi.org/10.36922/jctr.24.00044

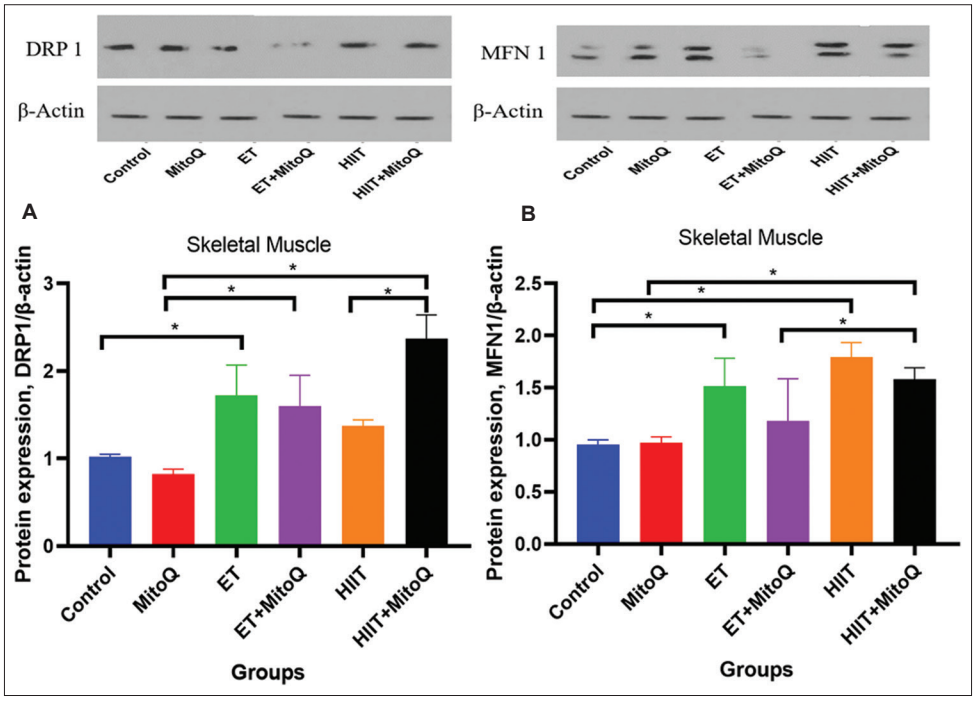

Figure 1. Protein expression of DRP1 in skeletal muscles. (A) DRP1 protein expression in different groups. (B) MFN1 protein expression in different groups. *$p < 0.05$
Abbreviations: ET: Endurance training; HIIT: High-intensity interval training

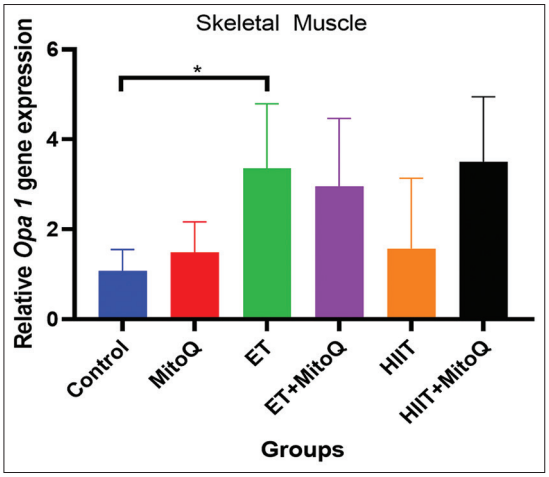

Figure 2. Quantitation of *Opa1* gene expression in skeletal muscles (mean ± SD). *$p < 0.05$
Abbreviations: ET: Endurance training; HIIT: High-intensity interval training

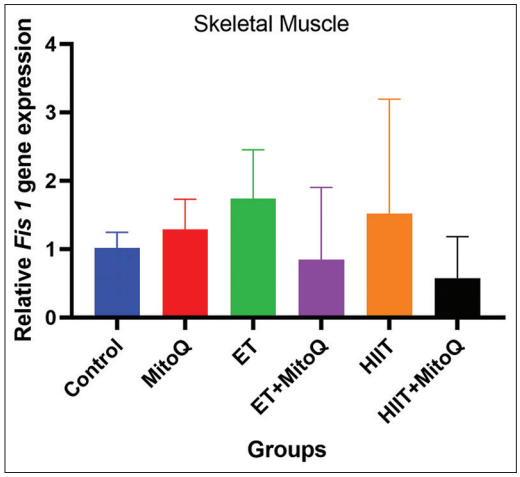

Figure 3. Quantitation of *Fis1* gene expression in skeletal muscles (mean ± SD)
Abbreviations: ET: Endurance training; HIIT: High-intensity interval training

exercise in the study of Yoo *et al.* [37] In their study, Axelrod *et al.* [38] showed that treadmill aerobic exercise (5 days/week, 12 weeks) did not significantly alter the expression of proteins related to the fusion of human muscles. OPA1 and mitofusins are related to mitochondrial fusion, which plays a pivotal role in muscle [34,39]. Furthermore, there are proteins, such as DRP1 and FIS1 which are involved in damaged mitochondria elimination through mitochondrial fission [39]. We showed that exercise, especially aerobic exercise training, caused a significant increase in the expression of MFN1 protein and *Opa1* gene. Axelrod *et al.* [38] also reported that aerobic exercise (12 weeks) significantly decreased the expression of proteins involved in mitochondrial fission (FIS1 and Parkin). Our data showed that aerobic training significantly increased the expression of DRP1 protein and has no effect on the expression of FIS1. The data of Axelrod *et al.*'s study [38] are not in line with our findings, probably due to the longer duration of exercise in their study and its implementation on human subjects [38]. It has been demonstrated that old mice exhibited increased protein expression of FIS1 and decreased level of MFN2, which

DOI: http://doi.org/10.36922/jctr.24.00044

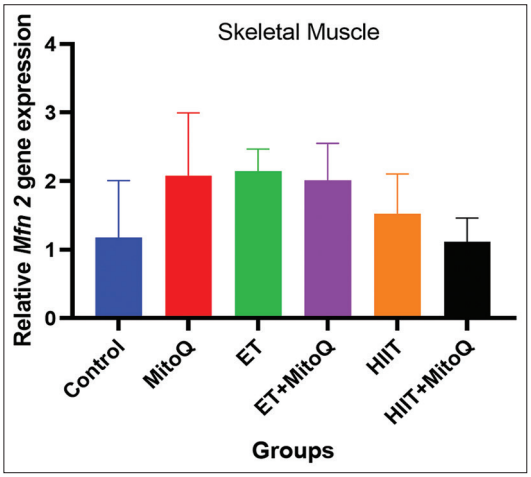

Figure 4. Quantitation of *Mfn2* gene expression in skeletal muscles (mean ± SD)
Abbreviation: ET: Endurance training; HIIT: High-intensity interval training

were reversible by exercise [40]. Ding *et al*. showed that after exercise, mitofusins and FIS1 expression increased in muscle compared to the other groups [33,38]. The results from our and Ding *et al*.'s studies confirm the inducing effect of exercise on mitochondrial fusion, along with the improvement of fission.

MitoQ is a targeted mitochondrial antioxidant that operates primarily by penetrating the mitochondrial membrane and selectively scavenging free radicals, thereby protecting mitochondrial function from oxidative damage. By delivering ubiquinone directly to the mitochondria, MitoQ enhances the electron transport chain's efficiency, leading to improved ATP production and energy metabolism. In addition, it has been shown to modulate mitochondrial dynamics by regulating key regulatory proteins involved in fission and fusion processes, thus maintaining optimal mitochondrial morphology and functionality [16-19]. The interplay between MitoQ and various physiological stimuli, such as exercise training, suggests a role in optimizing mitochondrial health, highlighting its potential as a therapeutic supplement in conditions characterized by mitochondrial dysfunction [20,35,40,41-43]. The MitoQ treatment prevented excessive mitochondrial fragmentation by regulating DRP1 phosphorylation. More importantly, MitoQ maintained aerobic respiration and reduced anaerobic respiration by regulating reprogramming of intracellular energy metabolism, which enhanced cellular ATP production [21]. In the current study, we did not observe any effect of ET alone on the MFN1 protein and *Opa1* gene expression when comparing this independent treatment with the combined ET + MitoQ regimen. On the other hand, we observed an increase in DRP1 protein level in both the ET and ET + MitoQ groups. It has been previously reported that mitochondrial adaptations following muscle exercise are not affected by MitoQ [35]. Furthermore, it has been reported that even though MitoQ augmented PGC-1α expression in muscles, the increase in mitochondrial content caused by exercise remained unaltered by MitoQ treatment [35]. Despite these studies, Williamson *et al*. [41] showed that MitoQ has a protective effect on the mitochondrial genome in muscle tissue post-exercise. In another study on human NP cells, they showed that administration of MitoQ decreased apoptosis and the expression of DRP1 and FIS1 while increasing the expression of proteins involved in fusion [42]. In our study, the administration of MitoQ neutralized the enhancing effects of ET on fusion, and in addition, in the rats that performed HIIT exercise, it enhanced fission by increasing the expression of DRP1 protein (in the HIIT + MitoQ group). These findings contradict the previous studies where MitoQ had no effect in the groups that performed exercise [42]. Given that exercise, particularly aerobic exercise influences the mitochondria and MitoQ specifically targets the mitochondria, the results in the ET + MitoQ and HIIT + MitoQ groups should align more closely with predictions. Despite the contradiction with other studies, it can be concluded that the duration of exercise, the target tissue, the way of MitoQ administration, and the dose of MitoQ are important factors that can affect the results. MitoQ ameliorates mitochondrial dysregulation in heart failure by attenuating hydrogen peroxide generation and increasing mitochondrial respiration [43]. It has also been reported that MitoQ administration reduces mitochondrial damage [44].

Moreover, the apparent discrepancy between our findings and previous studies can be attributed to several factors, including the duration of exercise, the specific muscle tissues examined, and the different methodologies employed for MitoQ administration [35,40]. For instance, previous literature has indicated that aerobic training can enhance mitochondrial function without necessarily altering dynamics [36], yet our study underscores that prolonged and specific exercise interventions, such as ET, can lead to significant changes in protein expression related to both fusion and fission processes [34]. In addition, the dynamic regulation of these proteins, such as DRP1's role in fission and MFN1 and OPA1's roles in fusion, highlights the bidirectional nature of mitochondrial adaptations to exercise [38]. Thus, a comprehensive exploration of how exercise influences mitochondrial dynamics, particularly in combination with specific pharmacological interventions like MitoQ, is essential to deepen our understanding of mitochondrial function in skeletal muscle. Future research should continue to investigate these interactions with varying exercise intensities and durations to elucidate the complexities of mitochondrial dynamics.

Limitations of the current study include the usage of a single MitoQ dose and the relatively short duration of MitoQ treatment. The dose and treatment duration employed in this study were based on the previous studies. In our experience, intraperitoneal injection of MitoQ to rats could be lethal; therefore, we administered it through the drinking water. The toxic effects of this supplement may be related to the role of mitochondria as stress sensors, and it can modulate nuclear functioning through retrograde signaling. Furthermore, another limitation of this research is the housekeeping gene/protein used, *that is*, β-actin. Since this study involves monitoring mitochondrial changes, housekeeping proteins like translocase of the outer membrane 22 or voltage-dependent anion channel and housekeeping gene like mitochondrial processing subunit alpha (*Pmpca*) should be used instead.

DOI: http://doi.org/10.36922/jctr.24.00044

5. Conclusion

The findings of this study highlight the differential impacts of exercise modalities, ET and HIIT, on mitochondrial quality control in skeletal muscle. Our results indicate that ET significantly enhances mitochondrial dynamics, evidenced by a robust increase in the expression levels of proteins linked to mitochondrial fusion and fission, specifically DRP1, MFN1, and OPA1. These adaptations underscore ET's superior capacity to improve mitochondrial function, which is crucial for muscle metabolism and performance. HIIT, while beneficial, primarily promoted mitochondrial fusion as indicated by the increase in MFN1 protein levels, suggesting a more focused impact on mitochondrial dynamics under anaerobic conditions. Interestingly, although MitoQ treatment alone did not elicit substantial changes in mitochondrial dynamics, its combination with exercise training shed light on their complex interactions: in combination with ET, MitoQ appeared to downregulate mitochondrial protein expression, whereas coupled with HIIT, it further enhanced DRP1 expression, suggesting the varying effects of this pharmacological intervention depending on the exercise modality. This finding is critical, as it implies that while MitoQ may support certain mitochondrial functions, its effects are context-dependent and highlight the necessity of investigating specific exercise protocols in conjunction with administration of mitochondria-targeted therapies.

To build a more comprehensive understanding of the mechanisms underlying these observations, further research is necessary. Future studies should explore varying doses and duration of MitoQ treatment to better elucidate its effects on mitochondrial dynamics and function across different exercise intensities. By expanding our examination of these interactions and understanding their implications for skeletal muscle physiology, we can advance the understanding of metabolic control and develop more effective interventions for enhancing mitochondrial health in various populations.

Acknowledgments

The authors would like to express their heartfelt gratitude to the Student Research Committee and the Vice Chancellor for Research and Technology at Kerman University of Medical Sciences for their invaluable support of our study.

Funding

This research was funded by the Vice Chancellor for Research and Technology of Kerman University of Medical Sciences, Kerman, Iran (Grant number: 98000779).

Conflicts of Interest

The authors declare no competing interest.

Author Contributions

Conceptualization: Beydolah Shahouzehi, Soheil Aminizadeh
Formal analysis: Beydolah Shahouzehi, Soheil Aminizadeh, Hamid Najafipour, Yaser Masoumi-Ardakani
Investigation: Beydolah Shahouzehi, Soheil Aminizadeh, Hamid Najafipour, Yaser Masoumi-Ardakani
Methodology: Beydolah Shahouzehi, Soheil Aminizadeh, Mohammad Pourranjbar
Writing – original draft: All authors
Writing – review & editing: All author

Ethics Approval and Consent to Participate

The animal procedure was approved by the guidelines of the Animal Care Committee of the Ethics Committee of Kerman University of Medical Sciences (IR.KMU.REC.1400.292). All methods were performed in accordance with the ARRIVE (Animal Research: Reporting of In Vivo Experiments) guidelines 2.0.

Consent for Publication

Not applicable.

Availability of Data

The datasets generated during and/or analyzed during the current study are available from the corresponding author on reasonable request.

References

[1] Karbowski M. Mitochondria on Guard: Role of Mitochondrial Fusion and Fission in the Regulation of Apoptosis. Adv Exp Med Biol 2010;687:131-42. doi: 10.1007/978-1-4419-6706-0_8

[2] Wu T, Li Z, Wei Y. Advances in Understanding Mechanisms Underlying Mitochondrial Structure and Function Damage by Ozone. Sci Total Environ 2023;861:160589. doi: 10.1016/j.scitotenv.2022.160589

[3] Memme JM, Erlich AT, Phukan G, Hood DA. Exercise and Mitochondrial Health. J Physiol 2021;599:803-17. doi: 10.1113/JP278853

[4] Meng Q, Su CH. The Impact of Physical Exercise on Oxidative and Nitrosative Stress: Balancing the Benefits and Risks. Antioxidants (Basel) 2024;13:573. doi: 10.3390/antiox13050573

[5] Scarpulla RC, Vega RB, Kelly DP. Transcriptional integration of mitochondrial biogenesis. Trends Endocrinol Metab 2012;23:459-66. doi: 10.1016/j.tem.2012.06.006

[6] Slavin MB, Khemraj P, Hood DA. Exercise, mitochondrial dysfunction and inflammasomes in skeletal muscle. Biomed J 2024;47:100636. doi: 10.1016/j.bj.2023.100636

[7] Sokolova I. Mitochondrial Adaptations to Variable Environments and their Role in Animals' Stress Tolerance. Integr Comp Biol 2018;58:519-31. doi: 10.1093/icb/icy017

[8] Jenner A, Pena-Blanco A, Salvador-Gallego R, Ugarte-Uribe B, Zollo C, Ganief T, *et al*. Drp1 Interacts Directly with Bax to Induce its Activation and Apoptosis. EMBO J 2022;41:e108587.
doi: 10.15252/embj.2021108587

[9] Bhat S, Chin A, Shirakabe A, Ikeda Y, Ikeda S, Zhai P, *et al*. Recruitment of RNA Polymerase ii to Metabolic Gene Promoters is Inhibited in the Failing Heart Possibly through PGC-1Alpha (Peroxisome Proliferator-activated Receptor-Gamma Coactivator-1Alpha) Dysregulation. Circ Heart Fail 2019;12:e005529.
doi: 10.1161/CIRCHEARTFAILURE.118.005529

[10] Gureev AP, Shaforostova EA, Popov VN. Regulation of Mitochondrial Biogenesis as a Way for Active Longevity: Interaction between the nrf2 and pgc-1alpha Signaling Pathways. Front Genet 2019;10:435.
doi: 10.3389/fgene.2019.00435

[11] Menezes TN, Ramalho LS, Bechara LR, Ferreira JCB. Targeting Mitochondrial Fission-fusion Imbalance in Heart Failure. Curr Tissue Microenviron Rep 2020;1:239-47.

[12] Youle RJ, Van der Bliek AM. Mitochondrial Fission, Fusion, and Stress. Science 2012;337:1062-5.
doi: 10.1126/science.1219855

[13] Hernandez-Resendiz S, Prunier F, Girao H, Dorn G, Hausenloy DJ, Action E-CC. Targeting Mitochondrial Fusion and Fission Proteins for Cardioprotection. J Cell Mol Med 2020;24:6571-85.

[14] Schrepfer E, Scorrano L. Mitofusins, from Mitochondria to Metabolism. Mol Cell 2016;61:683-94.
doi: 10.1016/j.molcel.2016.02.022

[15] Filadi R, Pendin D, Pizzo P. Mitofusin 2: From Functions to Disease. Cell Death Dis 2018;9:330.
doi: 10.1038/s41419-017-0023-6

[16] Ihenacho UK, Meacham KA, Harwig MC, Widlansky ME, Hill RB. Mitochondrial Fission Protein 1: Emerging Roles in Organellar form and Function in Health and Disease. Front Endocrinol (Lausanne) 2021;12:660095.
doi: 10.3389/fendo.2021.660095

[17] Mao P, Manczak M, Shirendeb UP, Reddy PH. MitoQ, a Mitochondria-targeted Antioxidant, Delays Disease Progression and Alleviates Pathogenesis in an Experimental Autoimmune Encephalomyelitis Mouse Model of Multiple Sclerosis. Biochim Biophys Acta 2013;1832:2322-31.
doi: 10.1016/j.bbadis.2013.09.005

[18] Tauskela JS. MitoQ--a Mitochondria-Targeted Antioxidant. IDrugs 2007;10:399-412.

[19] Pham T, MacRae CL, Broome SC, D'Souza RF, Narang R, Wang HW, *et al*. MitoQ and CoQ10 Supplementation Mildly Suppresses Skeletal Muscle Mitochondrial Hydrogen Peroxide Levels without Impacting Mitochondrial Function in Middle-aged Men. Eur J Appl Physiol 2020;120:1657-9.

[20] Sulaimon LA, Afolabi LO, Adisa RA, Ayankojo AG, Afolabi MO, Adewolu AM, *et al*. Pharmacological Significance of MitoQ in Ameliorating Mitochondria-Related Diseases. Adv Redox Res 2022;5:100037.
doi: 10.1016/j.arres.2022.100037

[21] Tsui KH, Li CJ. Mitoquinone Shifts Energy Metabolism to Reduce ROS-induced oxeiptosis in female granulosa cells and mouse oocytes. Aging (Albany NY) 2023;15:246-60.
doi: 10.18632/aging.204475

[22] Chen S, Wang Y, Zhang H, Chen R, Lv F, Li Z, *et al*. The Antioxidant MitoQ Protects Against CSE-induced Endothelial Barrier Injury and Inflammation by Inhibiting ROS and Autophagy in Human Umbilical Vein Endothelial Cells. Int J Biol Sci 2019;15:1440-51.
doi: 10.7150/ijbs.30193

[23] Merry TL, Ristow M. Do Antioxidant Supplements Interfere with Skeletal Muscle Adaptation to Exercise training? J Physiol 2016;594:5135-47.
doi: 10.1113/JP270654

[24] Moore TM, Zhou Z, Cohn W, Norheim F, Lin AJ, Kalajian N, *et al*. The impact of exercise on mitochondrial dynamics and the role of drp1 in exercise performance and training adaptations in skeletal muscle. Mol Metab 2019;21:51-67.
doi: 10.1016/j.molmet.2018.11.012

[25] Braakhuis AJ, Nagulan R, Somerville V. The Effect of MitoQ on Aging-related Biomarkers: A Systematic Review and Meta-analysis. Oxid Med Cell Longev 2018;2018:8575263.
doi: 10.1155/2018/8575263

[26] Zadeh HJ, Roholamini Z, Aminizadeh S, Deh-Ahmadi MA. Endurance Training and MitoQ Supplementation Improve Spatial Memory, VEGF Expression, and Neurogenic Factors in Hippocampal Tissue of Rats. J Clin Transl Res 2023;9:1-7.

[27] Hu J, Cai M, Shang Q, Li Z, Feng Y, Liu B, *et al*. Elevated Lactate by High-Intensity Interval Training Regulates the Hippocampal Bdnf Expression and the Mitochondrial Quality Control System. Front Physiol 2021;12:629914.
doi: 10.3389/fphys.2021.629914

[28] Verboven M, Cuypers A, Deluyker D, Lambrichts I, Eijnde BO, Hansen D, *et al*. High Intensity Training Improves Cardiac Function in Healthy Rats. Sci Rep 2019;9:5612.
doi: 10.1038/s41598-019-42023-1

[29] Batacan RB Jr., Duncan MJ, Dalbo VJ, Connolly KJ, Fenning AS. Light-intensity and High-intensity Interval Training Improve Cardiometabolic Health in Rats. Appl Physiol Nutr Metab 2016;41:945-52.
doi: 10.1139/apnm-2016-0037

[30] Pour MB, Joukar S, Hovanloo F, Najafipour H. Long-term Low-intensity Endurance Exercise Along with Blood-flow Restriction Improves Muscle Mass and Neuromuscular Junction Compartments in Old Rats. Iran J Med Sci 2017;42:569-576.

[31] Mohammadi A, Fallah H, Shahouzehi B, Najafipour H. Effect of LXR Agonist t0901317 and MIR-33inhibitor on SIRT1-AMPK and Circulating HDL-C levels. Bulg Chem Commun 2018;50:111-8.

[32] Jiang HK, Wang YH, Sun L, He X, Zhao M, Feng ZH, *et al*. Aerobic interval Training Attenuates Mitochondrial Dysfunction in Rats Post-myocardial Infarction: Roles of Mitochondrial Network Dynamics. Int J Mol Sci 2014;15:5304-22.
doi: 10.3390/ijms15045304

[33] Ding H, Jiang N, Liu H, Liu X, Liu D, Zhao F, *et al*. Response of mitochondrial Fusion and Fission Protein Gene Expression to Exercise in rat skeletal muscle. Biochim Biophys Acta 2010;1800:250-6.
doi: 10.1016/j.bbagen.2009.08.007

[34] Hood DA, Memme JM, Oliveira AN, Triolo M. Maintenance of skeletal muscle mitochondria in health, exercise, and aging. Annu Rev Physiol 2019;81:19-41.
doi: 10.1146/annurev-physiol-020518-114310

[35] Broome SC, Pham T, Braakhuis AJ, Narang R, Wang HW, Hickey AJR, *et al*. MitoQ Supplementation Augments Acute Exercise-induced Increases in Muscle pgc1α mRNA and Improves Training-induced Increases in Peak Power Independent of Mitochondrial Content and Function in Untrained Middle-aged Men. Redox Biol 2022;53:102341.
doi: 10.1016/j.redox.2022.102341

[36] Lee YJ, Jeong SY, Karbowski M, Smith CL, Youle RJ. Roles of the Mammalian Mitochondrial Fission and Fusion Mediators FIS1, DRP1, and OPA1 in Apoptosis. Mol Biol Cell 2004;15:5001-11.
doi: 10.1091/mbc.e04-04-0294

[37] Yoo SZ, No MH, Heo JW, Park DH, Kang JH, Kim JH, *et al*. Effects of Acute Exercise on Mitochondrial Function, Dynamics, and Mitophagy in Rat Cardiac and Skeletal Muscles. Int Neurourol J 2019;23:S22-31.
doi: 10.5213/inj.1938038.019

[38] Axelrod CL, Fealy CE, Mulya A, Kirwan JP. Exercise Training Remodels Human Skeletal Muscle Mitochondrial Fission and Fusion Machinery Towards a Pro-Elongation Phenotype. Acta Physiol (Oxf) 2019;225:e13216.
doi: 10.1111/apha.13216

[39] Hall AR, Burke N, Dongworth RK, Hausenloy DJ. Mitochondrial fusion and Fission Proteins: Novel Therapeutic Targets for Combating Cardiovascular disease. Br J Pharmacol 2014;171:1890-906.
doi: 10.1111/bph.12516

[40] Gioscia-Ryan RA, Battson ML, Cuevas LM, Zigler MC, Sindler AL, Seals DR. Voluntary Aerobic Exercise Increases Arterial Resilience and Mitochondrial Health with Aging in Mice. Aging (Albany NY) 2016;8:2897-914.
doi: 10.18632/aging.101099

[41] Williamson J, Hughes CM, Cobley JN, Davison GW. The Mitochondria-targeted Antioxidant MitoQ, Attenuates Exercise-induced Mitochondrial DNA Damage. Redox Biol 2020;36:101673.
doi: 10.1016/j.redox.2020.101673

[42] Kang L, Liu S, Li J, Tian Y, Xue Y, Liu X. The Mitochondria-targeted Anti-Oxidant MitoQ Protects Against Intervertebral Disc Degeneration by Ameliorating Mitochondrial Dysfunction and Redox Imbalance. Cell Prolif 2020;53:e12779.
doi: 10.1111/cpr.12779

[43] Ribeiro Junior RF, Dabkowski ER, Shekar KC, Connell KAO, Hecker PA, Murphy MP. MitoQ Improves Mitochondrial Dysfunction in Heart Failure Induced by Pressure Overload. Free Radic Biol Med 2018;117:18-29.
doi: 10.1016/j.freeradbiomed.2018.01.012

[44] Lowes DA, Webster NR, Murphy MP, Galley HF. Antioxidants that Protect Mitochondria Reduce Interleukin-6 and Oxidative Stress, Improve Mitochondrial Function, and Reduce Biochemical Markers of Organ Dysfunction in a Rat Model of Acute Sepsis. Br J Anaesth 2013;110:472-80.
doi: 10.1093/bja/aes577

Journal of Clinical and Translational Research

Journal of Clinical and Translational Research (JCTR) welcomes submissions from various research topics that are centered on solving clinically-driven issues to ultimately benefit patients.

You will benefit from the following key features of JCTR as our author:

- Open access
- Author-friendly guidelines: 'your paper, your way'
- Reputable editorial board
- No word count or reference restrictions
- Double-blind review process to minimize bias
- Rapid production and publication
- Broad scope, interdisciplinary research exchange platform

The research areas that JCTR covers include, but are not limited to:

Internal medicine (all branches)	Gastroenterology and hepatology
Vascular medicine and phlebology	Surgery and transplantation
Oncology	Hematology
Cardiology	Nephrology
Intensive care medicine	Dermatology
Ophthalmology	Endocrinology and metabolism
Neurology and neurosciences	Anesthesiology
Anatomy, physiology, and embryology	Radiology and nuclear medicine
Pathology	Clinical chemistry
Clinical physics	Genetics and epigenetics
Epidemiology	Global health
Medical devices	Nutrition
Pharmacology	Immunology
Microbiology	Virology
Parasitology	Biomedical engineering

Biomedical spectroscopy and spectrometry

Thanks for considering the Journal of Clinical and Translational Research.

Editorial team JCTR

Journal of Clinical and Translational Research is an independent open access journal published by ACCSCIENCE PUBLISHING

Contact: info@jctres.com • Tel: +65 8182 1586
www.jctres.com

ACCSCIENCE PUBLISHING

ACCSCIENCE PUBLISHING
8 Burn Road, #15-03 Trivex, Singapore 369977.
Tel: +65 8182 1586